

---

Electronic Thesis and Dissertation Repository

---

4-27-2015 12:00 AM

# Exploration of Spatial and Temporal Changes in Trophic Status of Lakes in the Northern Temporal Forest Biome Using Remote Sensing

Aleksey Paltsev, *The University of Western Ontario*

Supervisor: Dr. Irena I. Creed, *The University of Western Ontario*

A thesis submitted in partial fulfillment of the requirements for the Master of Science degree in Biology

© Aleksey Paltsev 2015

Follow this and additional works at: <https://ir.lib.uwo.ca/etd>



Part of the [Biodiversity Commons](#), [Biogeochemistry Commons](#), [Environmental Monitoring Commons](#), [Forest Biology Commons](#), [Fresh Water Studies Commons](#), [Hydrology Commons](#), [Other Earth Sciences Commons](#), [Other Oceanography and Atmospheric Sciences and Meteorology Commons](#), [Terrestrial and Aquatic Ecology Commons](#), and the [Water Resource Management Commons](#)

---

## Recommended Citation

Paltsev, Aleksey, "Exploration of Spatial and Temporal Changes in Trophic Status of Lakes in the Northern Temporal Forest Biome Using Remote Sensing" (2015). *Electronic Thesis and Dissertation Repository*. 2825.

<https://ir.lib.uwo.ca/etd/2825>

This Dissertation/Thesis is brought to you for free and open access by Scholarship@Western. It has been accepted for inclusion in Electronic Thesis and Dissertation Repository by an authorized administrator of Scholarship@Western. For more information, please contact [wlsadmin@uwo.ca](mailto:wlsadmin@uwo.ca).

EXPLORATION OF SPATIAL AND TEMPORAL CHANGES  
IN TROPHIC STATUS OF LAKES IN THE  
NORTHERN TEMPERAL FOREST BIOME USING REMOTE SENSING  
(Thesis format: Monograph)

by

Aleksey I. Paltsev

Graduate Program in Biology

A thesis submitted in partial fulfillment  
of the requirements for the degree of  
Master of Science

The School of Graduate and Postdoctoral Studies  
The University of Western Ontario  
London, Ontario, Canada

© Aleksey I. Paltsev 2015

## Abstract

There is a critical need for detailed surveys of lakes covering large spatial (>100 km<sup>2</sup>) and temporal scales (decades) to determine if there is an increase in the magnitude and frequency of phytoplankton blooms. Remote sensing was used to: (1) develop a regression model that relates chlorophyll a (chl-a) as a proxy of lake phytoplankton biomass to Landsat TM and ETM+ optical reflectance ( $r^2=0.85$ ,  $p<0.001$ ); and (2) apply this regression model to estimate chl-a in lakes within the Temperate Forest Biome in Ontario over a 28-year period. A two-way Analysis of Variance of remotely sensed chl-a of lakes revealed a spatial pattern of relatively low chl-a in headwater lakes to higher chl-a in lower reaches of watersheds, and a temporal pattern within a trend. These findings suggest that the recent increase in community-driven reports of phytoplankton blooms is not indicative of an actual increase in phytoplankton blooms in these lakes.

**Keywords:** temperate forest, lakes, trophic status, phytoplankton blooms, phytoplankton, chlorophyll a, remote sensing

## **Co-Authorship Statement**

Mr. Aleksey Paltsev will be the first author on any manuscript(s) submitted from the contents of this thesis as he conducted satellite imagery data processing, statistical analysis, and contributed to the design of the research approach. Dr. Irena F. Creed will be a co-author on any manuscript(s) submitted from the contents of this thesis as she contributed to the definition of the research problem, synthesis of ideas and interpretation of the research results.

Financial support of the research activities for this project was provided by Natural Sciences and Engineering Research Council of Canada (NSERC) Discovery Grants to Dr. Irena F. Creed.

## **Acknowledgments**

First of all, I would like to thank my supervisor, Dr. Irena Creed, for all of her guidance and encouragement throughout the entire 2.5 year research project. Dr. Creed is an amazing scientist whose dedication to my professional development has been invaluable and greatly appreciated.

I thank my advisory committee members, Dr. Katrina Moser, Dr. Hugh Henry and Dr. Brian Branfireun, for allowing me the opportunity to accomplish this goal. Each member of my advisory committee contributed bright ideas that were instrumental in making my thesis a success.

I thank Mr. David Aldred for his tremendous help in guiding me through remote sensing techniques and developing automated scripts for satellite image processing. I also thank Ms. Xue (Sherry) Qin for her incredible willingness to help as well as for her support with satellite image processing and Ms. Jacqueline Serran for her help with formatting text and numerous graphs in this thesis.

I would like to extend a special thanks to Dr. Eric Enanga who made my first field trip in Canada unforgettable and from whom I learnt a lot on soil sampling. I would also like to thank Dr. R. Sorichetti and Dr. G. Sass who became good friends of mine and who provided me with the precious field data I used in my research.

# Table of Contents

Abstract .....	ii
Co-Authorship Statement.....	iii
Acknowledgments .....	iv
Table of Contents .....	v
List of Tables .....	vii
List of Figures.....	viii
Chapter 1 .....	1
1 Introduction .....	1
1.1 Problem Statement.....	1
1.2 Theoretical framework for optical remote sensing of phytoplankton.....	3
1.3 Analytical framework for optical remote sensing of phytoplankton .....	11
1.4 Hypothesis and Objectives.....	13
1.5 Thesis Organization.....	13
Chapter 2 .....	15
2 Study Region.....	15
Chapter 3 .....	18
3 Methods .....	18
3.1 Ground-based data.....	18
3.2 Satellite-based data.....	19
3.2.1 Rationale for choosing Landsat TM and ETM+ imagery .....	19
3.2.2 Landsat data acquisition .....	19
3.2.3 At-satellite radiance calibration.....	20
3.2.4 Atmospheric correction .....	20
3.2.5 Lake identification .....	24
3.2.6 Lake selection for regression modeling .....	25
3.2.7 Regression modeling .....	26
3.2.8 Decomposition of variance .....	27
Chapter 4 .....	29
4 Results .....	29
4.1 Chl-a concentration in ground-based samples.....	29
4.2 Regression model.....	29
4.2.1 Results validation.....	34
4.3 Spatial patterns in modelled chlorophyll a.....	34
4.4 Temporal patterns in modelled chlorophyll a .....	37
4.5 Alterations in the trophic status of lakes.....	37
4.6 Decomposition of total variation into space, time and space × time components .....	40
Chapter 5 .....	45
5 Discussion.....	45
5.1 Regression model analysis .....	45

5.2. Analysis of spatial and temporal patterns .....	45
Chapter 6 .....	51
6 Conclusions.....	51
References .....	53
Curriculum Vitae.....	62

## List of Tables

<b><u>Table 1.1:</u></b> Overview of Landsat satellite sensors for phytoplankton monitoring (past and currently operational) modified from Chander <i>et al.</i> (2009). RBV: Return Beam Vidicon; MSS: Multispectral Scanner System; TM: Thematic Mapper; ETM+: Enhanced Thematic Mapper; OLI: Operational Land Imager; pan: panchromatic; IR: infrared; NIR: near infrared; SWIR: shortwave infrared; TIR: thermal infrared. ....	7
<b><u>Table 1.2:</u></b> Overview of remote sensing studies using Landsat imagery for the estimation of different parameters in inland waters only. B: Landsat band number; LR: simple linear regression; MLR: multiple linear regression; Chl-a: chlorophyll-a; SD: Secchi disk depth; TURB: turbidity; TSS: total suspended sediment; TSM: total suspended matter; DOM: dissolved organic matter.....	9
<b><u>Table 3.1:</u></b> Correspondence between Landsat image capture dates and ground measurement dates. ....	21
<b><u>Table 4.1:</u></b> Descriptive statistics of in situ lake physical, chemical and biological data. ....	30
<b><u>Table 4.2:</u></b> Pearson correlation coefficients between <i>in situ</i> DOC and various Landsat bands, band ratios, and band combinations. ....	32



## List of Figures

<b><u>Figure 1.1:</u></b> Evidence for the increased number of phytoplankton blooms in southern Ontario (modified from Winter <i>et al.</i> , 2011). .....	2
<b><u>Figure 2.1:</u></b> Location of the study region in the Temperate Forest Biome of Ontario and the location of sampled lakes. ....	16
<b><u>Figure 3.1:</u></b> Flowchart of Landsat TM and ETM+ image processing steps, lake identification and reflectance calculation. ....	22
<b><u>Figure 4.1:</u></b> Pearson correlation coefficients ( $r$ ) between $CHLa_{obs}$ ( $\ln [\mu\text{g } CHLa_{obs}/L]$ ) and various Landsat bands, band combinations and band ratios.....	31
<b><u>Figure 4.2:</u></b> Relationship of time window between <i>in situ</i> and satellite observations and $r^2$ , and number of lakes.....	33
<b><u>Figure 4.3:</u></b> Scatter-plot of B3 reflectance regressed against $CHLa_{obs}$ ( $\ln [\mu\text{g } CHLa_{obs}/L]$ ).....	35
<b><u>Figure 4.4:</u></b> Comparison of $CHLa_{obs}$ ( $\ln [\mu\text{g } CHLa_{obs}/L]$ ) and $CHLa_{mod}$ ( $\ln [\mu\text{g } CHLa_{mod}/L]$ ).....	36
<b><u>Figure 4.5:</u></b> Map of average $CHLa_{mod}$ ( $\mu\text{g}/L$ ) for 21,384 lakes in a 28-year record....	38
<b><u>Figure 4.6:</u></b> Time series of median $CHLa_{mod}$ ( $\ln [\mu\text{g } CHLa_{mod}/L]$ ) for 6,384 lakes in a 28-year record (1984-2011) with an additional axis for $CHLa_{mod}$ ( $\mu\text{g}/L$ ).....	39
<b><u>Figure 4.7:</u></b> Comparison in distribution of trophic status of lakes (%) for two ten-year periods (1985-1994 and 1995-2004).....	41
<b><u>Figure 4.8:</u></b> Sources of natural variation of $CHLa_{mod}$ ( $\ln [\mu\text{g } CHLa_{mod}/L]$ ).....	42
<b><u>Figure 4.9:</u></b> Number of years needed to establish the stability of variance in $CHLa_{mod}$ ( $\ln [\mu\text{g } CHLa_{mod}/L]$ ).....	43
<b><u>Figure 4.10:</u></b> Number of lakes needed to establish the stability of variance in $CHLa_{mod}$ ( $\ln [\mu\text{g } CHLa_{mod}/L]$ ).....	44

## List of Abbreviations

chl-*a*: Chlorophyll *a*

CHL*a*<sub>obs</sub>: Observed (sampled in the field) chlorophyll-*a*

CHL*a*<sub>mod</sub>: Modelled chlorophyll-*a*

DOC: Dissolved organic carbon

TM: Landsat Thematic Mapper sensor

ETM+: Landsat Enhanced Thematic Mapper sensor

OLI: Operational Land Imager sensor

B1: Band 1 (Landsat blue band)

B2: Band 2 (Landsat green band)

B3: Band 3 (Landsat red band)

B4: Band 4 (Landsat near infrared band)

ANOVA: Analysis of variance

RMSE: Root mean square error

DOS - Dark Object Subtraction method

COST: Cosine of Sun Zenith Angle variation of DOS method

## Chapter 1

### 1 Introduction

#### 1.1 Problem Statement

Lakes in the temperate forests of eastern North America appear to be experiencing an increase in the frequency and duration of phytoplankton blooms. These blooms are often comprised of phytoplankton species that have the capacity to produce toxic secondary metabolites such as neurotoxins, hepatoxins and gastrotoxins that can cause serious health problems for animals and humans (Havens, 2008). This has been the focus of numerous recent public and government reports (Winter *et al.*, 2011), resulting in heightened public concern and public reporting of phytoplankton blooms in Ontario (Figure 1.1).

Phytoplankton blooms have usually been associated with the process of eutrophication where excess macronutrients such as phosphorus (P) and nitrogen (N) enter water bodies (Paerl and Huisman, 2009). The leading cause of this excessive nutrient concentration is mainly ascribed to anthropogenic influences through either direct discharge of waste products and chemical fertilizers into surface waters (Glibert *et al.*, 2005) or widespread land use and land cover change (e.g. deforestation, prairie plowing, wetland drainage, etc.) (Foley *et al.*, 2005). However, these explanations provide little or no insight into phytoplankton bloom occurrence in nutrient poor oligotrophic lakes located on relatively pristine landscapes a considerable distance from urban zones and agricultural lands.

Canada's Great Lakes-St. Lawrence forest region contains 18% of the world's freshwater resources. With relatively little anthropogenic influence in the northern parts of this region, it is likely that other factors are contributing towards a rise in phytoplankton biomass. For example, climate warming and associated hydrological and biogeochemical changes may be contributing to increased phytoplankton biomass in oligotrophic lakes (O'Neil *et al.*, 2012). More intense precipitation events promote washing of nutrients out from uplands to wetlands and lakes, increasing their nutrient enrichment. On the other hand, the prolonged periods of droughts lead to the effect when nutrients are captured within lakes, raising a possibility of blooms (Paul, 2008; Paerl and Paul, 2012).

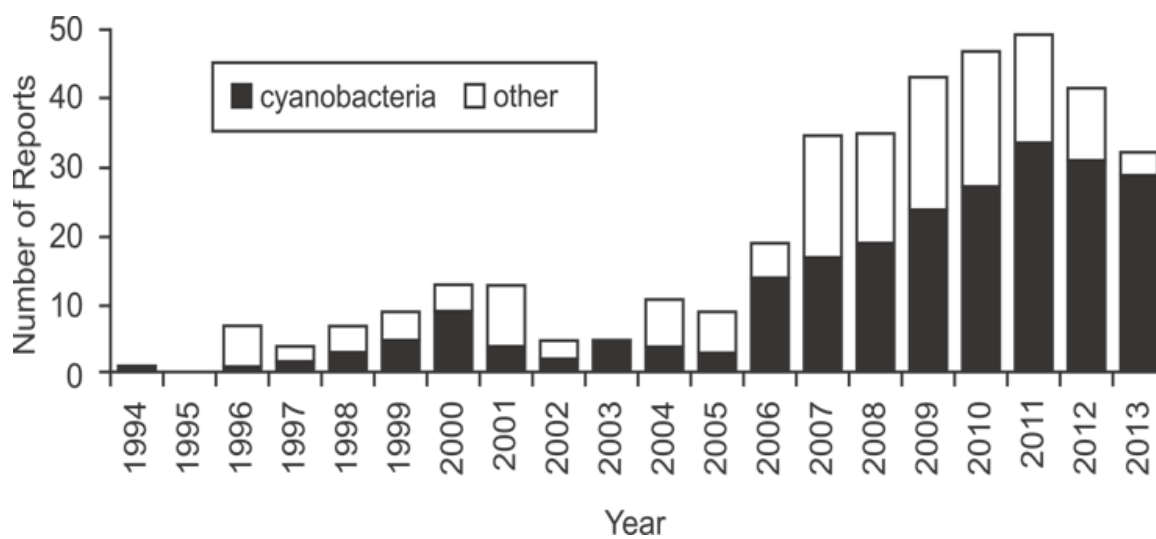


**Figure 1.1:** Evidence for the increased number of phytoplankton blooms in southern Ontario (modified from Winter *et al.*, 2011).

It should also be noted that heightened awareness of phytoplankton blooms may indicate perceived rather than real concerns. An increased number of reports does not necessarily indicate an actual increase in phytoplankton blooms. Public perception may be heightened by a greater number of news stories illustrated with photographs of dead fish and livestock. Therefore, there is a critical need for a detailed historical survey of lake phytoplankton biomass covering large regional scales over extended periods (decades) that can help determine whether global factors such as climate change do play an important role and whether public perceptions are accurate.

Until recently it was unfeasible to conduct this kind of research because it required both comprehensive historical records and laborious sampling campaigns in frequently difficult-to-access locations. The era of remotely sensed imagery, however, allows for characterization of lake phytoplankton over large spatial extents over the past several decades.

## **1.2 Theoretical framework for optical remote sensing of phytoplankton**

Satellite remote sensing has proven to be an effective tool for ecological research in inland water bodies, helping to understand past and current complex ecological and biogeochemical processes occurring in them. In lake science, the application of remote sensing is based on the inherent properties of water, its dissolved components, and phytoplankton pigments to absorb or reflect solar radiation at specific wavelengths within the electromagnetic spectrum (Richardson, 1996).

The ability of a surface to reflect radiation is measured by reflectance; i.e., the ratio of the total amount of reflected radiation (light) to the total amount of radiation (light) incident on the surface. Every dissolved component or pigment in water has its own reflectance properties, making it possible to “trace” their presence and concentration in the water column. Phytoplankton detection is possible through the optical properties of one of the principal pigments of all phytoplankton, chlorophyll *a* (chl-*a*). Some phytoplankton groups have specific pigments, such as phycocyanin in cyanobacteria with an electromagnetic absorption peak at about 620 nm, meaning that these groups can be distinguished from other phytoplankton by their reflectance (Kallio, 2012). Since cyanobacteria in most cases are responsible for both

phytoplankton bloom development and toxin production (Downing *et al.*, 2001), remote sensing promises to be a useful technique for studying these blooms via detection of phycocyanin concentration in water. However, this technique is hampered by the inability of most satellite sensors to resolve the narrow bandwidths of these specialized absorption peaks and is still under investigation (Vincent *et al.*, 2004).

Among several currently existing remote sensing systems, one of the most popular and widely available systems is the Landsat satellite series. It offers the longest continuous record of satellite-based observations of the Earth's surface starting with the launch of the first satellite in the series (Multispectral Scanner or MSS) in the early 1970s (Fraser 1998). Landsat Thematic Mapper (TM) and Enhanced TM (ETM+) sensors were subsequently launched to provide finer spatial resolution (30 m). Landsat TM and ETM+ images consist of seven spectral bands (with one additional band for ETM+) (Table 1.1). Table 1.1 presents an overview of all past and currently operational Landsat satellite sensors.

Landsat TM and ETM+ have a long history of successful quantification of phytoplankton chl-a (Carpenter and Carpenter, 1983; Lathrop *et al.*, 1991; Gitelson, 1992; Fraser, 1998; Allee and Johnson, 1999; Svab *et al.*, 2005; Cannizzaro and Carder, 2006; Karakaya *et al.*, 2011; McCullough *et al.*, 2012; Hicks *et al.*, 2013; Giardino *et al.*, 2014). These studies relied mostly on: (1) the optical properties of chl-a characterized by low reflectance in the red wavelengths and high reflectance in the near-infrared; and (2) simple linear or multiple linear regression models where satellite measured reflectance was related statistically to near-simultaneous ground-based measurements of chl-a.

The successful use of Landsat TM and ETM+ imagery depends on various factors, including the methods used for: (1) ground-based data collection (e.g., depth from which a sample was collected); (2) correction of raw Landsat images to remove terrain and atmospheric effects; and (3) statistical analysis (e.g., the type of regression analysis used) (Liu *et al.*, 2003; Kallio, 2012). It has also been shown that estimates produced by regression models can be highly dependant on chl-a concentration; accuracy can significantly drop with decreasing chl-a concentration (El-Alem *et al.*, 2012).

A review of existing literature of inland lake parameter models developed from remotely sensed imagery (using Landsat in particular) revealed that the majority of models were developed from a single lake (e.g., Ritchie *et al.*, 1990; Mayo *et al.*, 1995; Budd and Warrington, 2004; Vincent *et al.*, 2004; Tebbs *et al.*, 2013; Rodríguez *et al.*, 2014), some from a few lakes (e.g., Dekker and Peters, 1993; Gitelson, 1993; Baruah *et al.*, 2001; Brezonik *et al.*, 2005), and only a handful from a large number of lakes (e.g., Chipman *et al.*, 2004; Olmanson *et al.*, 2013) (Table 1.2). Few studies have attempted to estimate chl-a over a period of more than one year (e.g., Kloiber *et al.*, 2002; Sass *et al.*, 2007; McCullough *et al.*, 2012; Hicks *et al.*, 2013) (Table 1.2).

The studies that aimed at the model developing from many lakes transferred knowledge from a few representative lakes to many lakes in a region. They used *in situ* measurements from a few representative lakes to calibrate relationships between Landsat TM or ETM+ imagery and chl-a, then extended the scale of study from one year to decades and/or from small to large regions. For example, Pulliainen *et al.* (2001) predicted average chl-a concentration for lakes in southern Finland using regression models developed from ground-based chl-a measurements in just six lakes. The authors found that average chl-a can be reliably estimated from satellite data (AISA hyperspectral system) without having *in situ* measurements for every lake. Sass *et al.* (2007) classified trophic status in 76 lakes in northern Alberta (Canada), finding a relationship between Landsat TM Band 3 (red) reflectance and ground observations from 18 lakes ( $r^2 = 0.68$ ,  $p < 0.0001$ ). Further, they used the regression equation and the reflectance derived from archived TM data to build a time series of chl-a concentration for 20 years, thereby confirming the possibility of using remote sensing of the lakes with no *in situ* data for continuous temporal analysis. Allan *et al.* (2011) characterized the spatial and temporal distribution of chl-a in numerous lakes spread over the large area of the Central Volcanic Plateau in New Zealand, finding a strong relationship between Landsat ETM+ Band 3 reflectance values and *in situ* data ( $r^2 = 0.95$ ,  $p < 0.001$ ). The developed model was transferred to predict the concentration of chl-a for two different seasons (spring and summer) of the same year. The previously mentioned studies have one particular idea in common: their models were developed for the same biogeoclimatic and physiographic region.

**Table 1.1:** Overview of Landsat satellite sensors for phytoplankton monitoring (past and currently operational) modified from Chander *et al.* (2009). RBV: Return Beam Vidicon; MSS: Multispectral Scanner System; TM: Thematic Mapper; ETM+: Enhanced Thematic Mapper; OLI: Operational Land Imager; pan: panchromatic; IR: infrared; NIR: near infrared; SWIR: shortwave infrared; TIR: thermal infrared.

Satellite	Sensors	Launch Date	Decommission Date	Resolution			Altitude (km)	
				Spectral Bands (B) (nm)		Pixel Size (m)		Revisit Period (days)
Landsat 1	MSS and RBV	July 23, 1972	January 7, 1978	RBV B1 (green): 480-570	MSS B4 (green): 500-600 B5 (red): 600-700	80 (RBV) 79 (MSS)	18	920
Landsat 2	MSS and RBV	January 22, 1975	February 25, 1982	B2 (red): 580-680 B3 (NIR): 700-830	B6 (NIR): 700-800 B7 (SWIR): 800-1,100	80 (RBV) 79 (MSS)	18	920
Landsat 3	MSS and RBV	March 5, 1978	March 31, 1983	RBV B1 (pan): 505-750	MSS B4 (green): 500-600 B5 (red): 600-700 B6 (NIR): 700-800 B7 (SWIR): 800-1,100 B8 (TIR): 10,400-12,600	40 (RBV) 79 (MSS) 240 (MSS thermal)	18	920
Landsat 4	MSS and TM	July 16, 1982	June 30, 2001	MSS B4 (green): 500-600	TM B1 (blue): 450-520 B2 (green): 520-600 B3 (red): 630-690	82 (MSS) 30 (TM)	16	705
Landsat 5	MSS and TM	March 1, 1984	Completely deactivated: June 5, 2013	B5 (red): 600-700			16	705



				B6 (NIR): 700-800 B7 (SWIR): 800-1,100	B4 (NIR): 760-900 B5 (SWIR-1): 1,550-1,750 B6 (thermal IR): 10,400-12,500 B7 (SWIR-2): 2,080-2,350			
Landsat 6	ETM+	October 5, 1993	Did not achieve orbit	B1 (blue): 450-520 B2 (green): 520-600 B3 (red): 630-690 B4 (NIR): 760-900 B5 (SWIR-1): 1,550-1,750 B6 (TIR): 10,400-12,500 B7 (SWIR-2): 2,080-2,350 B8 (pan): 500-900			16	705
Landsat 7	ETM+	April 15, 1999	Operational			30 120 (thermal) 15 (pan)	16	705
EO-1	OLI	November 21, 2000	Operational	B1 (coastal aerosol): 433-453 B2 (blue): 450-515 B3 (green): 525-600 B4 (red): 630-680 B5 (NIR): 845-885 B6 (SWIR-1): 1,560-1,660 B7 (SWIR-2): 2,100-2,300 B8 (pan): 500-680 B9 (cirrus): 1,360-1,390 B10 (TIR-1): 10,600-11,200 B11 (TIR-2): 11,500-12,500		30 100 (TIR) 15 (pan)	16	705

**Table 1.2:** Overview of remote sensing studies using Landsat imagery for the estimation of different parameters in inland waters only. B: Landsat band number; LR: simple linear regression; MLR: multiple linear regression; Chl-a: chlorophyll-a; SD: Secchi disk depth; TURB: turbidity; TSS: total suspended sediment; TSM: total suspended matter; DOM: dissolved organic matter.

Public ation	Location	Sensor	# of modeled lakes	# of years (period)	Lake parameter	Statistical technique	Bands/band combinations/ band ratios	r <sup>2</sup> (chl-a only)	Reference
2013	USA, Minnesota	TM, ETM+	10500	20 (1985– 2005)	SD	MLR	B1/B3	n/a	Olmanson <i>et al.</i> (2013)
2013	New Zealand, theWaikato region	ETM+	34	9 (2000– 2009)	TSS, SD	LR	B4, B3, B1/B3	n/a	Hicks <i>et al.</i> , 2013
2012	USA, Maine	TM, ETM+	1511	20 (1990– 2010)	SD	LR (forward stepwise regression)	B1/B3	n/a	McCullough <i>et al.</i> (2012)
2011	New Zealand, Central Volcanic Plateau	ETM+	n/a	1 (2001)	Chl-a	LR	B3, B1/B3	0.95	Allan <i>et al.</i> (2011)
2008	Southern Finland	ETM+	n/a	1 (2002)	SD, TURB, DOM	LR	B1/B3	n/a	Kallio <i>et al.</i> (2008)
2007	Canada, Alberta, Boreal Plain	TM, ETM+	76	20 (1984– 2003)	Chl-a, SD, TURB	LR	B3	0.68	Sass <i>et al.</i> (2007)
2004	USA, Wisconsin	TM, ETM+	8645	3 (1999– 2001)	SD	MLR	B1/B3, B1	n/a	Chipman <i>et al.</i> (2004)
2003	USA, lower peninsula of Michigan	ETM+	93	1 (2001)	SD	LR	B1/B3	n/a	Nelson <i>et al.</i> (2003)

2003	USA, Minnesota	TM	94	1 (2001)	SD	MLR	B1/B3, B1	n/a	Sawaya <i>et al.</i> (2003)
2002	USA, Minnesota, Twin Cities Metropolitan Area	TM, MSS	64–170	25 (1973– 1998)	SD	step-wise regression, MLR	B1/B3, B1	n/a	Kloiber <i>et al.</i> (2002)
2002	The Netherlands, Southern Frisian Lakes	TM	n/a	n/a	TSM	Analytical	$(B2 + B3)/2$	n/a	Dekker <i>et al.</i> (2002)
2001	Southern Finland	TM	85	1 (1997)	Chl-a, SD, TURB	LR	B1/B2, B1–B4)/ (B3– B1– B4)/(B3– B4), (B1– B4)/(B3– B4)	n/a	Härmä <i>et al.</i> (2001)
1998	USA, Nebraska Sand Hills, Nebraska	TM	21	1 (1994)	TURB	LR	B3	n/a	Fraser (1998)

### 1.3 Analytical framework for optical remote sensing of phytoplankton

For this research the framework developed by Wiley *et al.* (1997) and later applied by Sass *et al.* (2007) was adapted. Figure 1.2 shows schematic (A) and statistical (B) models of three types of variation (space, time and space  $\times$  time interaction components) that contribute to overall variance in chl-a concentration. Conceptually, the spatial component represents variation due to landscape attributes of a study region including geology, topography, hydrology, forest and soil type (c.f. Devito *et al.*, 2005). Data on these attributes should be spatially extensive (Wiley *et al.*, 1997). For instance, they cannot represent concentration of chl-a for a single lake but rather for many lakes in the region. The temporal component represents variation due to differences between years including climatic oscillations and trends as well as human development. Finally, the space  $\times$  time interaction component represents non-synchronous site (lake) specific variation in time. Processes leading to this type of variation occur within lakes and can be biological (e.g., interactions between species including competition and predation) or physical (e.g., morphometric properties of lakes such as lake area, depth, size of littoral zone). The complexity of processes involved in this type makes it difficult to define what exactly causes the variation. Therefore, Sass *et al.* (2007) called it "variation due to unknown factors".

Statistically, all three components are integrated into the paradigm of standard two-way analysis of variance (ANOVA). ANOVA has been widely used in ecological research for evaluating spatial and temporal patterns with applications for zooplankton (Lewis, 1978), fish and insect populations (Wiley *et al.*, 1997), and chl-a of eutrophic lakes (Sass *et al.*, 2007). The spatial component represents averaged time variation between sites, the temporal component represents averaged spatial variation between years, while the space  $\times$  time interaction component accounts for interaction between time and space variations, namely variations that are site-specific (e.g. chl-a that varies across the lakes of the same study region). Finally, the error term in the ANOVA analysis may also be found in the space  $\times$  time interaction component. This error is associated with any measurement or remote sensing processing errors. It is possible to separately estimate the errors (i.e., not have them included in the space  $\times$

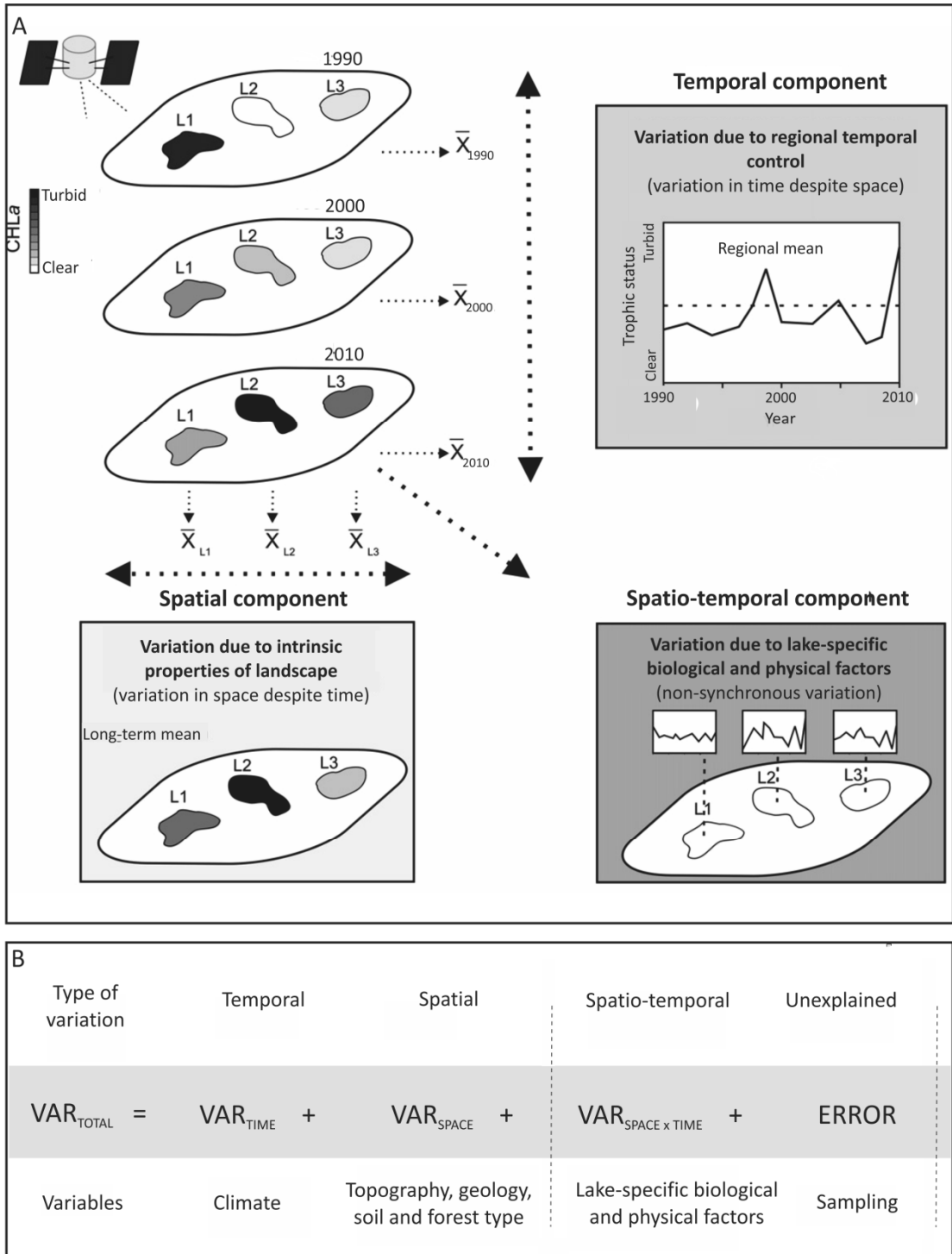


**Figure 1.2:** Schematic (A) and statistical (B) models of variation in the trophic status of lakes (modified from Sass *et al.*, 2007).

time interaction component), but only if any replicates were collected during the sampling period (Wiley *et al.*, 1997).

## 1.4 Hypothesis and Objectives

The goal of the research is to characterize spatial and temporal variation in lake chl-a as a proxy of phytoplankton biomass of lakes in the study region (the northern edge of the Temperate Forest Biome) in Ontario.

The hypothesis is that concentration of chl-a in lakes in the Temperate Forest Biome of Ontario is highly dependent on spatial and temporal differences in topography and climatic patterns. The predictions are that: (1) the temporal component of variation in chl-a is large, with an increase in chl-a over time related to climate change; (2) the spatial component of variation in chl-a is similarly large, with a systematic pattern of increase in chl-a from the upper to lower reaches of watersheds; and (3) the space  $\times$  time interaction component of variation is the smallest.

To test this hypothesis, the following objectives were completed:

1. develop regression models that relate chl-a to optical reflectance;
2. apply these models to estimate chl-a concentration in lakes over several decades;
3. decompose the total variation in chl-a into space, time, and space  $\times$  time interaction components to identify the main factors influencing chl-a concentration.

The results of the study will help to identify which factors are associated with reported phytoplankton blooms and allow researchers to target future monitoring efforts on the potentially susceptible lakes in forested landscapes.

## 1.5 Thesis Organization

This thesis has been prepared in monograph format. The introduction (Chapter 1) provides an overview of the research problem and presents the theoretical and analytical approaches to address the research problem. Chapter 2 outlines the study region. The methods section (Chapters 3) describes methods used in the study. Chapter 4 describes the findings of the research, while these findings are discussed in

detail in Chapter 5 with particular emphasis on the spatial and temporal factors influencing variation in chl-a. Chapter 6 summarises the major conclusions of the work, discusses the anticipated significance of the study, and identifies future research directions.

## Chapter 2

### 2 Study Region

The study region is in the Great Lakes-St. Lawrence Forest region located at the northern edge of the Temperate Forest Biome and confined by the administrative borders of the province of Ontario (Figure 2.1).

Climate is continental, with precipitation being influenced by lake effect from the Great Lakes and local orographic effects in areas of high relief (Baldwin *et al.*, 2011). According to McKenney *et al.* (2011), mean annual precipitation in the study region for the period of 1981–2010 was 990 mm. Areas with maximum annual precipitation are located along topographic heights facing the Great Lakes, especially in the Batchawana and Muskoka watersheds (1135 mm and 1150 mm respectively). Average annual mean air temperature for 1981–2010 was +4.4 °C, varying between +7.0 °C in the south-east and 1.8 °C in the north (McKenney *et al.*, 2011). The frost-free period greatly depends on the location; in more warm and humid south regions this period normally extends from April to November while in the north it lasts from May to September (Baldwin *et al.*, 2011). Peaks in stream discharge occur during snowmelt in March to April and again in September to November during autumn storms (Mengistu *et al.*, 2013).

Geology is the Precambrian rocks of the Canadian Shield. Bedrock geology is primarily composed of silicate greenstone with small outcrops of more felsic igneous rock (Ontario Geological Survey, 2003). In the south, these rocks are almost completely covered with glaciofluvial outwash, whereas they come to the surface throughout the Algoma Highlands and the north portion of the study region. The outwash is 1–2 m in width and generally consists of two layers: sandy loam ablation till and a compacted lower slit loam basal till (Ontario Geological Survey, 2003). Topography varies from flats and depressions along the shores of lakes Superior and Huron to hills and uplands (Algoma and Madawaska highlands, Batchawana Mountains). Elevations range from 180 m to 650 m at the summit of Batchawana Mountain with an average of 460 m (Baldwin *et al.*, 2000). The most rugged topography occurs in the Algoma Highlands where hills of mostly oblong forms with gentle to steep slopes drain into numerous wetlands and lakes.



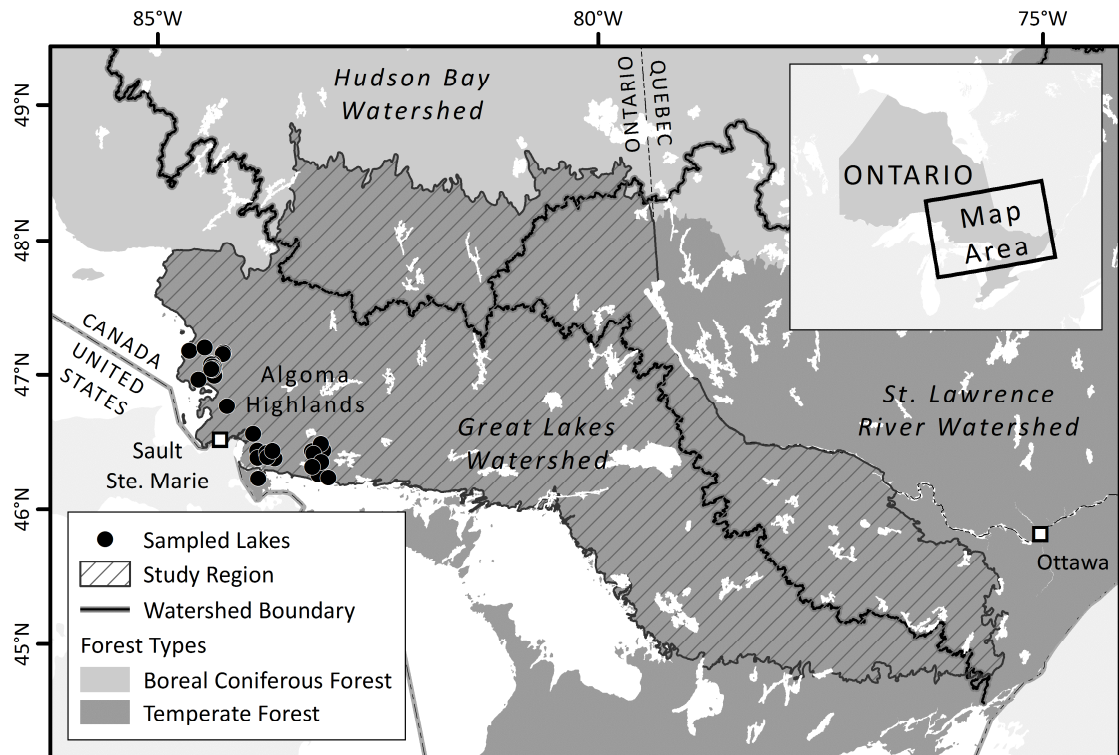


**Figure 2.1:** Location of the study region in the Temperate Forest Biome of Ontario and the location of sampled lakes.

Soils in the southern portion of the study region are thin and undifferentiated brunisols. Central and northern areas of the study region are represented by orthic ferro-humic podzols gradually thickening, differentiating, and increasing in organic content on topographic benches. Wetland areas are comprised of ferric humisols with highly humified organic deposits (Canada Soil Survey Committee, 1978).

The Great Lakes-St. Lawrence Forest region is the second largest forest region in Ontario and represents the transitional zone between deciduous and coniferous forests. Deciduous species are primarily comprised of sugar (*Acer saccharum* Marsh.) and red (*Acer rubrum* L.) maples, yellow birch (*Betula alleghaniensis* Britt.), and red oak (*Quercus rubra* L.). Coniferous species are represented by white (*Pinus strobes* L.) and red (*Pinus resinosa* Ait) pine, and eastern white cedar (*Thuja occidentalis* L.). There is a long history of forest management activities that have resulted in a fairly simple forest structure, with reduced species diversity and little variety in forest age (Carleton, 2000). In addition, logging has also led to significant changes in nutrient composition of local soils (especially nitrogen [N] and dissolved organic carbon [DOC]) that could have had potential impact on the streams and lakes of the study region (Kreutzweiser *et al.*, 2008).

## Chapter 3

### 3 Methods

#### 3.1 Ground-based data

Ground-based measurements were taken as a part of the field campaign launched in 2008 and conducted by Sorichetti (2013b). The measurements of chlorophyll *a* and DOC were made in 31 oligotrophic lakes in the Algoma Highlands of Ontario from 2009 to 2011 (Figure 2.1). Lakes were selected on a basis of minimal direct anthropogenic influence and public concern about the potential of phytoplankton blooms in the lakes. The sampled lakes are relatively deep (ranging between 0.8 m to 42.7 m; Sorichetti, 2013b), thermally stratified during the warm summer months, and dimictic with major mixing events occurring during the spring snowmelt and fall storms. Lakes were sampled at their centers throughout the ice-free season (May – October). Surface water samples integrated to 1.0 m depth were collected in 500 mL pre-rinsed polyethylene bottles near the centres of the lakes. The samples were then put into in a cooler with ice until return to the field laboratory.

Each sample was filtered onto Whatman GF/F filters and analysed for chl-*a* concentration according to EPA Method 445.0 (Arar and Collins, 1997). Chl-*a* was extracted from filters using an acetone/ultra-pure water solvent (90:10 v/v) in 20 mL scintillation vials and stored in the dark at -20 °C for 20 h. Samples were brought to room temperature in the dark and measured using a Turner 10-AU field fluorometer with a 680-nm emissions filter (Turner Designs, Sunnyvale, CA, U.S.A.).

Ground-based measurements of chl-*a* conducted by Sass *et al.* (2007) were also used in this study. The measurements were taken in 22 eutrophic lakes in August 2001 in the Boreal Plain in northern Alberta. The lakes were relatively shallow with an average depth of 1.3 m (Sass *et al.*, 2008). Lakes were sampled at their centers in mid-August coinciding with the summer peak in phytoplankton biomass. Grab samples were taken from a depth of 0.20-0.40 m of the water column and transported to a laboratory. Samples were filtered within 12 hours of collection, frozen, and later analyzed for chl-*a* using a spectrophotometer at 750, 665 and 649 nm using EPA Method 446.0 following the methods of Bergmann and Peters (1980) and Sass *et al.*

(2007). Satellite reflectance values for the Alberta lakes were also provided by Sass *et al.* (2007).

## 3.2 Satellite-based data

### 3.2.1 Rationale for choosing Landsat TM and ETM+ imagery

Archived Landsat TM and ETM+ satellite images were chosen as the source of satellite-based data for this research for a number of reasons: (1) well-established methods of image and associated metadata processing; (2) near-continuous coverage of archived satellite imagery starting from 1982; (3) global coverage allowing for analysis over large areas as well as in areas with limited or no physical access; and (4) free distribution, an especially important consideration for historic surveys of large areas with requirements of hundreds thousands of scenes.

### 3.2.2 Landsat data acquisition

Twelve Worldwide Reference System ground tracks (path and row combinations 22/27, 21/28, 20/27, 20/28, 17/28, 17/29, 16/29, 18/28, 18/29, 21/27, 19/27, 19/28; UTM zones 16, 17 and 18) were identified for the study region. Landsat TM (1984-2011) and ETM+ (1999-2003) scenes as well as associated metadata corresponding to these tracks were retrieved from US Geological Survey archives for the period of 1984-2011. ETM+ images for the period of 2003-2011 were not acquired due to a system failure in the Landsat 7 sensor in 2003 that resulted in wide strips of missing data within images. Only those images were selected that: (1) contained less than 50% cloud or haze cover; and (2) were captured from late July to early November. This period coincides with the peak phytoplankton biomass known for the study region, extending into a prolonged autumn boundary. This boundary may extend into ice cover periods, but it was set this way intentionally due to new evidence that duration of phytoplankton blooms is increasing, covering a period up to mid-November (Winter *et al.*, 2011).

Although the 16-day revisit period of Landsat satellites offers the potential to acquire two images for each ground track in most months, the presence of cloud cover limited this number; in many months no usable images could be acquired. Particular attention was paid to images captured from 2009 to 2011 – the period for which *in*

*situ* measurements of chl-a were available. A time window between image capture and ground observation within +/- 7 days was used to limit the search. Although this window is the longest period in which reasonable results can be yielded (Kloiber et al, 2002; Nelson *et al.*, 2003), it remained a challenge to find cloud-free Landsat images falling within this window.

A total of 1,067 Landsat TM and 159 ETM+ images were retrieved. Five images coinciding with the *in situ* measurements in 2009, 2010 and 2011 within +/- 6 days were acquired (Table 3.1). All images were corrected for terrain at delivery. Landsat images were imported into ArcGIS 10.2 where they were cropped to remove “dark” or zero value pixels on image margins. Only Bands 1-5 (out of 7) were processed and used in this analysis.

### 3.2.3 At-satellite radiance calibration

Landsat images are stored in 8-bit Digital Numbers (DNs) for the purpose of minimizing storage volume. This storage process involves scaling and offsetting the physical at-satellite radiance values (the amount of energy sensed by the satellite measured in  $W m^{-2} sr^{-1} \mu m^{-1}$ ). The first step in image analysis is to convert DN<sub>s</sub> for each image Band 1-4 back to at-satellite radiance values ( $L_{sat}$ ) using Equation 1:

[1]

where B and G are published post-launch image gain and bias provided in image metadata (Chander *et al.*, 2009). An automated script was developed for implementation in ArcGIS 10.2 to execute at-satellite radiance calibration. Figure 3.1 shows a flowchart of Landsat processing.

### 3.2.4 Atmospheric correction

Estimating phytoplankton biomass or other water quality variables from Landsat images depends on being able to relate Landsat pixel values to inherent physical optical properties of the variables. Because these physical properties do not vary in space or time, Landsat images acquired over a span of time and across different ground tracks must be corrected to a common radiometric scale in order to do quantitative analysis.

**Table 3.1:** Correspondence between Landsat image capture dates and ground measurement dates.

Date of image capture	Sensor	Ground measurement date
May 22, 2009	TM	May 17, 2009
June 12, 2009	TM	June 13, 2009
June 23, 2009	TM	June 24, 2009
June 17, 2010	TM	June 16, 2010
August 16, 2010	TM	August 16, 2010
July 31, 2011	TM	July 27, 2011

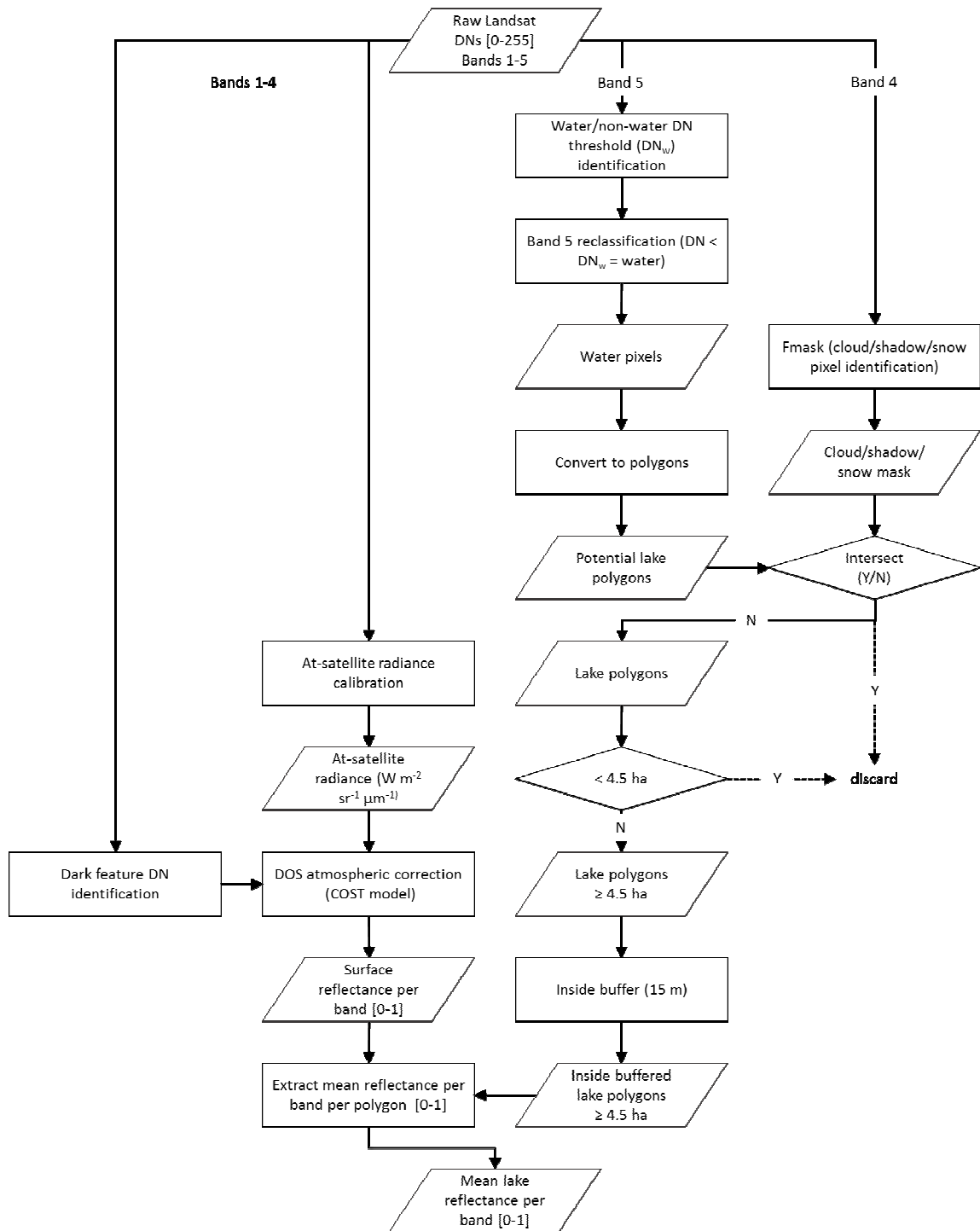


**Figure 3.1:** Flowchart of Landsat TM and ETM+ image processing steps, lake identification and reflectance calculation.

A major source of error is the modification of electromagnetic radiation signals collected by satellites from scattering and absorption by gases and aerosols as the signals travel through the atmosphere from the Earth's surface. Atmospheric interference can be particularly significant over water bodies, because interference increases as reflected radiance from water decreases (Brezonik *et al.* 2005). Atmospheric conditions vary in both space and time. The effects of atmospheric conditions depend on the wavelength of energy reaching the given satellite sensor. The main atmospheric effect is scattering which is additive to the remote sensed signals, while the effect of absorption is multiplicative.

A number of methods have been developed to correct satellite images for atmospheric effects (Chavez, 1996; Chen *et al.*, 2005). Physical models are the most complex and require detailed knowledge of atmospheric conditions such as Rayleigh atmosphere, aerosols and ozone optical depth at the time of image acquisition. As these parameters are rarely available – especially for historic and rural archived imagery – physical models can typically only be used for field-calibrated studies where *in situ* measurements can be made.

Relative methods use histogram matching and regression techniques to normalize images to a single reference image by selecting pseudo-invariant ground features (PIFs) that are assumed to have constant reflectance properties (Schott *et al.*, 1988; Furby *et al.*, 2001). Relative methods are not applicable when generalization of spectral features takes place across more than one Landsat frame as PIFs cannot be identified across ground tracks (Mahiny *et al.*, 2007).

Dark Object Subtraction methods (DOS) can be used across different scenes and do not require *in situ* atmospheric measurements. These methods assume that there are near-zero reflectance features ("dark features") within an image (e.g., clear water bodies, dense forest, shadows) and that the signal recorded by the sensor is solely a result of atmospheric scattering (path radiance) – this value is subtracted from all pixels in an image (Shunlin *et al.*, 2001). The Cosine of Sun Zenith Angle model (COST) variation of DOS was adopted for this study (Chavez, 1996).

“Dark feature” DNs ( $DN_{\min}$ ) were identified by examining a histogram of DNs in each image band. Only Bands 1-4 were processed and used in this analysis. The lowest DN with a count of at least 1,000 pixels (McDonald *et al.*, 1998) was recorded.



For each Landsat band, the COST equation normalizes for variations due to Earth-Sun distance and solar zenith angle in addition to atmospheric effects by converting physical at-satellite radiance values ( $L_{sat}$ ) to unitless [0-1] surface reflectance values ( $\rho$ ) using Equation 2 (Chavez, 1996):

$$\rho = \frac{\pi \times d^2 \times (L_{sat} - L_p)}{T_v \times (E_{sun} \times \cos \theta_z \times T_z + E_{down})} \quad [2]$$

where:

- a)  $d$  is the earth-sun distance in astronomical units (provided in lookup tables according to image capture date);
- b)  $L_p$  is dark object radiance ( $(L_p = DN_{min} - B / G)$  minus radiance contributed by a percentage of surface reflectance (0.01 (1%) is an assumption of dark object surface reflectance for Bands 1-3; 0.001 (0.1%) for Band 4; and 0 (0%) for Band 5 (Lu *et al.*, 2002; Mather and Tso, 2009; Clark *et al.*, 2010));
- c)  $T_v$  is atmospheric transmittance from target to sensor (assumed to be 1 by Lu *et al.*, 2002);
- d)  $E_{sun}$  is an exoatmospheric solar constant (provided in lookup tables according to satellite sensor);
- e)  $\theta_z$  is solar zenith angle in radians (published in image metadata); and
- f)  $T_z$  is atmospheric transmittance in the illumination direction from sun to target (given as  $\theta_z$  for Bands 1-4).

An automated script was developed for implementation in ArcGIS 10.2 to execute atmospheric correction for all images.

### 3.2.5 Lake identification

Pixels representing water bodies were identified according to an approach suggested by Frazier *et al.* (2003). A threshold value between water and non-water pixels for each image was identified by analysing histograms of raw Band 5 (shortwave infrared) DNs for each image (a band in which radiation is strongly absorbed by water). This value was then used to reclassify the Band 5 images where pixels were assigned as water below this threshold and values equal to and above the threshold were assigned as non-water.

Water pixels were then converted to polygons. Since the water pixels accounted for not only lakes but also for other water features such as rivers and streams, these polygons were manually removed, thereby leaving only lakes (the “satellite lakes”) for further analysis.

Cloud/shadow masks were generated automatically from the raw Landsat DNAs by applying a stand-alone software package Fmask 3.2 (“Function of Mask”) that was initially developed by Zhu and Woodcock (2012) as a Matlab code. Fmask uses the physical properties of clouds (e.g., temperature, brightness) and the darkening effect of cloud shadows in the near infrared band (Band 4) to separate cloud/shadow pixels and clear sky pixels. Fmask can also be used to detect snow pixels – this function was particularly important for analyzing images captured in late October – November. Lake polygons intersecting any pixels classified as cloud, shadow or snow were discarded.

### **3.2.6 Lake selection for regression modeling**

Sass *et al.* (2007) cite the importance of lake selection criteria when dealing with prediction of chl-a for small lakes because of potential errors appearing in pixels near or along lake shorelines. The reflectance properties of shallow water and/or abundant emergent or aquatic vegetation that appear at the edges of water features are different than those of deeper water, producing pixels with mixed reflectances.

In order to avoid this problem, a minimum lake area of 4.5 ha (50 digital pixels for images with 30 m resolution) was applied – lake polygons with a smaller area were discarded. The remaining lake polygons were buffered inside to a distance of 15 m (1/2 pixel distance), further reducing the potential effects of mixed pixels. Mean reflectance values for each Landsat Band 1-4 were extracted within each buffered lake polygon.

Twenty-six of 31 ground sampled lakes were matched with satellite lakes, meaning that seven ground sampled lakes were either: (1) cloud covered at the time of image capture; (2) smaller than 4.5 ha; or (3) image capture fell outside the +/-7 day window of ground observation. Nine of the 26 ground sampled lakes had *in situ* chl-a data for more than one image date within the +/- 7 day time window, resulting in a

total sample size of 35 Ontario lakes. All ground sample dates were found to fall within a +/- 6 day time window of image capture.

### 3.2.7 Regression modeling

Ground-based measurements of chl-a were related to mean lake reflectance. Pearson correlation was used to determine statistical relationships between natural log transformed ground-based chl-a (hereafter referred to as  $CHLa_{obs}$ ) and reflectances from Landsat bands (B), band combinations and band ratios. Band combinations and band ratios were chosen on the basis of a review of studies (Dekker and Peters, 1993; Chen *et al.*, 1996; Vincent *et al.*, 2004; Hellweger *et al.*, 2004). Twenty-one different bands, band combinations and band ratios were tested to determine the strongest relationship of reflectance to chl-a by comparing with  $CHLa_{obs}$  using the Pearson product-moment correlation coefficient ( $r$ ). This correlation had already been conducted on the  $CHLa_{obs}$  from the Alberta lakes.

The Pearson correlation coefficient was also used to test potential relationships between natural log transformed DOC sampled in the Ontario lakes and reflectance values to determine whether DOC had any confounding effect on reflectance.

Sass *et al.* (2007) found that a maximum +/- 2 day time window between ground measurement and image capture was optimal for their model. To determine this window for the Ontario lakes, simple linear regressions between reflectance (in the band, band combination or band ratio determined to have the strongest relationship with  $CHLa_{obs}$ ) and  $CHLa_{obs}$  for each time window interval step of one day between +/- 1 to +/- 6 days. A maximum +/- 3 day time window left a total of 31 Ontario lake samples.

Ontario and Alberta ground sampled lakes were combined into a single dataset for modeling. Cook's distance of  $CHLa_{obs}$  was calculated in three iterations to identify and eliminate six outliers, leaving 47 samples for use in modeling. The resulting dataset was randomly split into two datasets of 24 and 23 lakes covering approximately the same ranges of chl-a and reflectance in the band, band combination or band ratio determined to have the strongest relationship with  $CHLa_{obs}$ . The first dataset was used for model development and the second for model validation.

A linear regression model was developed from the first dataset of 24 lakes using  $CHLa_{obs}$  as the dependent variable and the band, band combination or band ratio determined to have the strongest relationship with  $CHLa_{obs}$  as the independent variable. The equation obtained from the regression model was applied to predict chl-a (hereafter referred to as  $CHLa_{mod}$ ) for the lakes in the model validation dataset. A linear regression was conducted using  $CHLa_{obs}$  from the validation dataset as the dependent variable and  $CHLa_{mod}$  as the independent variable to determine the strength of the model and to confirm that predicted values fit onto a 1:1 line with no intercept with observed values. The model equation was then applied to all lakes in each Landsat image and for the entire period of 1984-2011. These remaining images included 793 cloud-free processed images from the end of July to mid-November with the highest number of them captured in August and September (around 70%).

A total of 21,384 satellite lake observations were found to be located within the study region over the 28-year period. These lakes were used for evaluating spatial distribution of  $CHLa_{mod}$  within the study region as well as for analysing their trophic status. However, many of these lakes lacked complete  $CHLa_{mod}$  data for some years due to haze and clouds. In order to build temporal patterns where the development of chl-a over a 28-year period could be identified, it was important to have a continuous annual record of  $CHLa_{mod}$  for the same lakes. Therefore, lakes with missing data (i.e. missing years) were excluded, leaving a final selection of 6,384 lakes.

### **3.2.8 Decomposition of variance**

Two-way analysis of variance (ANOVA) was used to evaluate spatial and temporal patterns in  $CHLa_{mod}$  (Figure 1.2B). The variation in  $CHLa_{mod}$  was decomposed into space, time and space  $\times$  time interaction components, statistically expressed as the sum of squares in space ( $SS_{space}$ ), time ( $SS_{time}$ ), and space  $\times$  time ( $SS_{space \times time}$ ). The ANOVA matrix consisted of 28 columns corresponding to the number of years and 6,384 rows corresponded to the number of lake records. The space factor accounted for evaluation of the difference between the 28-year average  $CHLa_{mod}$  for a specific lake and the 28-year average of all lakes, whereas the time factor accounted for the difference between the average  $CHLa_{mod}$  of all lakes for a specific year and for the 28-year average of all lakes. The space  $\times$  time factor

estimated the difference between the total variation and the sum of variation in the space and time factors ( $SS_{\text{total}} - SS_{\text{space}} - SS_{\text{time}}$ ).

ANOVAs were also conducted on subsets of the dataset to examine the stability of variance in  $CHLa_{\text{mod}}$  with gradually increasing temporal and spatial extent of sampling (i.e., the effect of number of years and number of lakes). Twenty subsets were selected for testing both the number of years and the number of lakes. While testing the effect of the number of years: (a) ANOVAs were performed for every year from 1985 to 1997 and for every two years from 1998 to 2011; and (b) all 20 subsets consisted of 6,384 lakes. While testing the effect of the number of lakes: (a) ANOVAs were performed on subsets containing between 200 and 6384 lakes increasing in size by increments of 200 between 200 and 2000 lakes and of 400 between 2001 and 6384 lakes; and (b) all 20 subsets consisted of 28 years. In the end, two final datasets were created (number of years and number of lakes) with proportions of total variation in  $CHLa_{\text{mod}}$  (in percentages).

The minimum number of years and lakes which was required to establish the stability of variance in  $CHLa_{\text{mod}}$  was determined by identifying breakpoints for each of three components (i.e., space, time and time x space interaction) with the use of nonlinear piecewise regressions. Since the breakpoints for each component were different, the one with maximum value (i.e., number of years or number of lakes) was selected. At this breakpoint all these components were becoming stable.

## Chapter 4

### 4 Results

#### 4.1 Chl-a concentration in ground-based samples

CHL<sub>a</sub><sub>obs</sub> in 24 lakes selected for the regression model development ranged from 0.50 to 78.79 µg/L with an average of 14.51 µg/L (Table 4.1). CHL<sub>a</sub><sub>obs</sub> in the 23 lakes selected for the validation dataset ranged from 0.39 to 59.6 µg/L with an average of 12.1 (µg/L). This indicates that both datasets represented the lakes of all trophic states from oligotrophic to hypereutrophic (very nutrient rich; Carlson and Simpson, 1996).

#### 4.2 Regression model

Analysis of reflectance values showed that bands B2 (green) and B3 as well as band combinations B3\*B1 and B3\*B2 were significantly correlated to CHL<sub>a</sub><sub>obs</sub> in the Ontario lakes with B3 showing the strongest correlation ( $r=0.91$ ,  $p < 0.0001$ ; Figure 4.1). Similar coefficients were found by Sass *et al.* (2007) for Alberta lakes (B3,  $PCC = 0.82$ ,  $p < 0.0001$ ). Therefore, this band was chosen for the regression model development. It was interesting to find that band ratio B3\*B1 also had significant correlation reaching a mark of 0.90 ( $p < 0.0001$ ). There were no previous studies found having any comparable results for this ratio for inland waters.

The possible contribution of DOC to the strength of the regression model was considered. DOC absorbs moderately in the red wavelengths (B3) leading to potential changes in the spectral reflectance properties (Gitelson *et al.*, 1993, Svab *et al.*, 2006). However, there was no significant relationship found between this band and DOC ( $r = 0.38$ ,  $p = 0.18$ ,  $n = 14$ ; Table 4.2).

A series of linear regression models were developed of CHL<sub>a</sub><sub>obs</sub> from the Ontario lakes and B3 by successively increasing the time window between the day of image capture and sample day in one day increments from +/- 1 to +/- 6 days (Figure 4.2). As the time window increased, the strength of relationships decreased ( $r^2$  decreasing from 0.82 to 0.21 with increasing time windows). There was a significant drop in the strength of relationships after +/-3 days ( $r^2$  decreasing from 0.73 for +/- 3 days to 0.35 for +/- 4 days). The former finding agrees with the results achieved

**Table 4.1:** Descriptive statistics of *in situ* lake physical, chemical and biological data.

	<b>n</b>	<b>Mean</b>	<b>Min</b>	<b>Max</b>	<b>Median</b>
CHL <sub>a</sub> <sub>obs</sub> (µg/L)*	24	14.51	0.50	78.79	3.71
DOC (µg/L)	14	5148.68	2634.00	8477.90	4368.26
Validation CHL <sub>a</sub> <sub>obs</sub> (µg/L)	23	12.1	0.39	59.60	5.59

\* Final lake selection used for the regression model

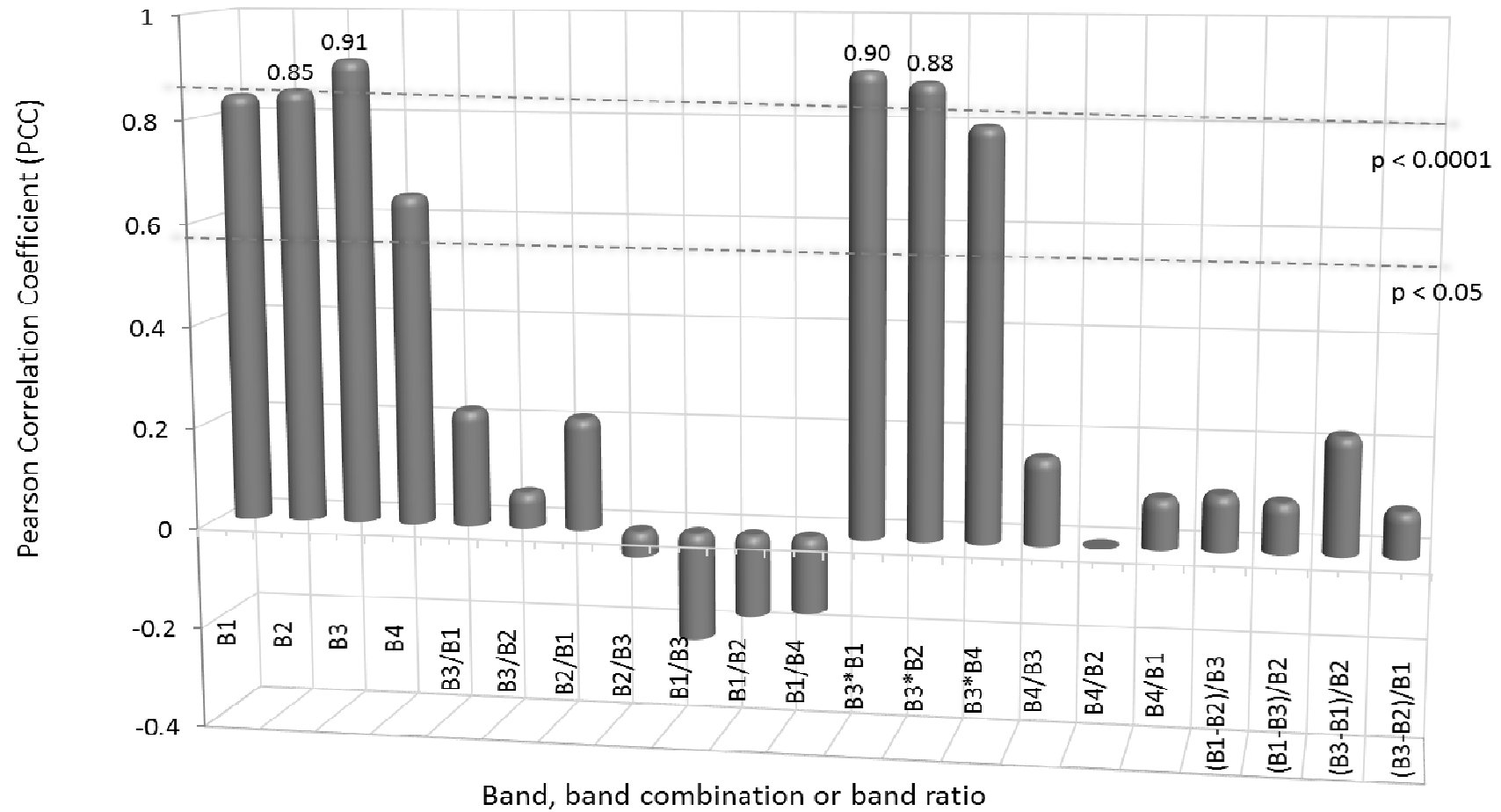


**Figure 4.1:** Pearson correlation coefficients ( $r$ ) between  $\text{CHLa}_{\text{obs}}$  ( $\ln [\mu\text{g CHLa}_{\text{obs}}/\text{L}]$ ) and various Landsat bands, band combinations and band ratios.



**Table 4.2:** Pearson correlation coefficients ( $r$ ) between *in situ* DOC and various Landsat bands and band ratios.

<b>Landsat band/band combination</b>	<b>B1</b>	<b>B2</b>	<b>B3</b>	<b>B3*B1</b>	<b>B3*B2</b>
DOC, n=14	0.42	0.29	0.38	0.39	0.18

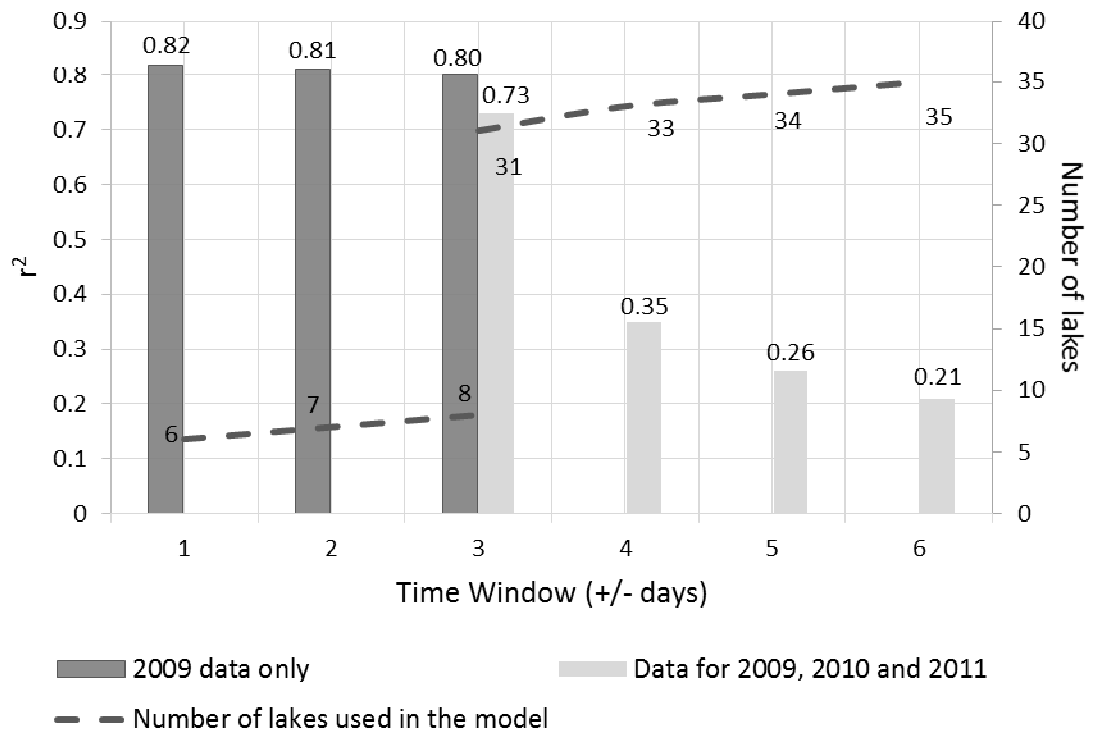


**Figure 4.2:** Relationship of time window between *in situ* and satellite observations and  $r^2$ , and number of lakes.

by Kloiber *et al.* (2001); however, these authors did not find a significant drop in the strength of their models from one time step to another owing likely to a far larger sample size (160 lakes in contrast to 35). Given the relative strength of the relationship found using a time window of +/- 3 days, the decision was made to use this time window to preserve a relatively large number of sample lakes (31).

Cook's distance identified six outliers in our dataset. Four of them came from Ontario dataset from 2011, while two came from the Alberta dataset. The fact that all the outliers from the Ontario dataset were from the same year suggests that this year may have been exceptional in terms of climatic conditions.

A linear regression model performed using  $CHLa_{obs}$  from the 24 lake model development dataset explained 85% of variation in  $CHLa_{mod}$  ( $r^2 = 0.85$ ,  $p < 0.001$ ,  $n = 24$ ; Figure 4.3). 23 out of 24 lakes fell within the bounds of 95% prediction limits.

#### 4.2.1 Results validation

The accuracy of model was assessed using the validation dataset of 23 lakes (Table 4.1). The comparison revealed significant correlation between  $CHLa_{obs}$  and  $CHLa_{mod}$  with a root mean square error (RMSE) = 0.55 ( $r^2 = 0.84$  and  $p < 0.0001$ ; Figure 4.4). The slope of the regression was found to be only slightly greater than 1 (1.0079) and the intercept only slightly less than 0 (-0.0997). Therefore, it was concluded that the predictive power of the model was good.

### 4.3 Spatial patterns in modelled chlorophyll a

Spatial patterns were assessed on the basis of a trophic status map of 21,384 lakes (Figure 4.5). The map was created by averaging the 28-year record of  $CHLa_{mod}$  for each lake. This average concentration was used to classify the lakes into four main trophic groups according to Carlson and Simpson (1996): oligotrophic, mesotrophic (intermediate nutrient levels), eutrophic (nutrient rich) and hypereutrophic. The map revealed two distinct patterns in average  $CHLa_{mod}$ .

First, lakes located in close proximity (within 100 km) to Lakes Superior and Huron are mostly mesotrophic or eutrophic. Further, most of the highly productive hypereutrophic lakes ( $CHLa_{mod} > 56 \mu\text{g}$ ) of the study region are also found in close proximity to the Great Lakes (especially to the northern shore of Lake Huron and Saul Ste. Marie metropolitan area). This trend is less obvious in the south-eastern portion

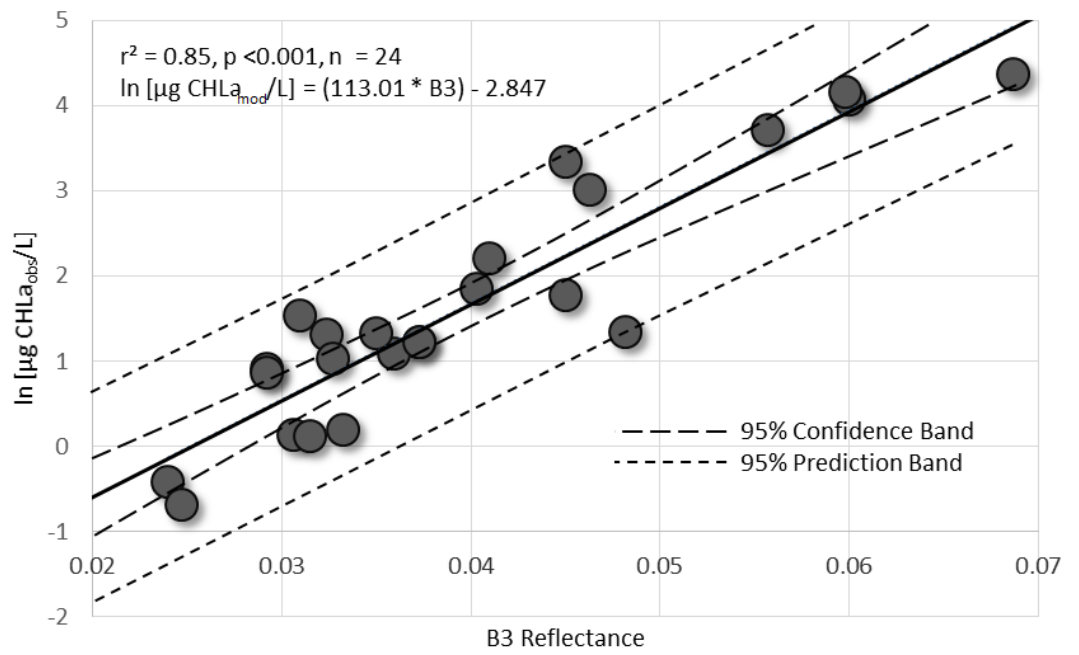


**Figure 4.3:** Scatter-plot of B3 reflectance regressed against  $\text{CHLa}_{\text{obs}}$  ( $\ln [\mu\text{g CHLa}_{\text{obs}}/\text{L}]$ ).

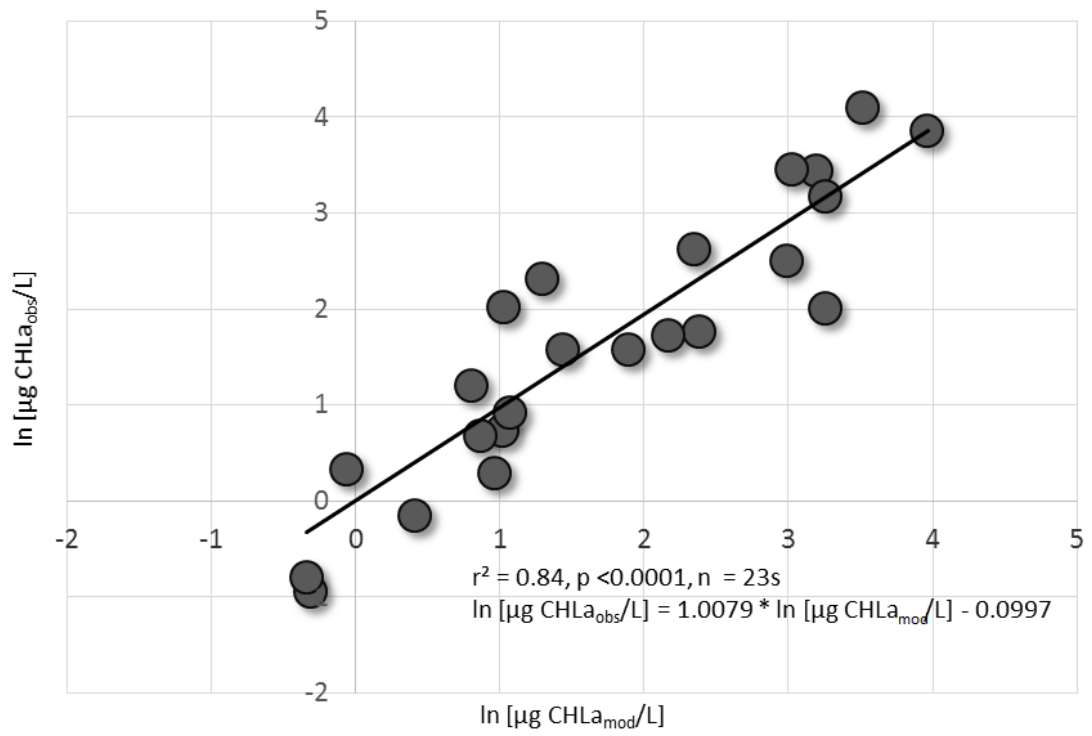


**Figure 4.4:** Comparison of CHLa<sub>obs</sub> (ln [µg CHLa<sub>obs</sub>/L]) and CHLa<sub>mod</sub> (ln [µg CHLa<sub>mod</sub>/L]).

of the region. The distribution of mesotrophic and eutrophic lakes is apparently more random.

Second, oligotrophic lakes are concentrated along the topographic divides between watersheds. They form an almost continuous "oligotrophic belt" with the only interruption in the south-eastern portion of the region.

#### **4.4 Temporal patterns in modelled chlorophyll a**

A 28-year time series of annual median  $CHLa_{mod}$  for 6,384 lakes was created for the analysis of temporal patterns (Figure 4.6).

The time series revealed a cyclic structured pattern in the median  $CHLa_{mod}$  with a different range and intensity of fluctuation over the 28-year period. The range of fluctuation seems to be higher between 1989 and 1999. The time series also revealed three peaks in the median  $CHLa_{mod}$  in 1991, 2000 and 2010 with approximately the same  $CHLa_{mod}$  (7.5  $\mu\text{g/L}$ ).

#### **4.5 Alterations in the trophic status of lakes**

The bar chart of comparison in the proportions of lakes trophic status for two periods showed an increasing trend in the proportion of lakes with high level of biological production (Figure 4.7). The proportion of oligotrophic lakes decreased from 49.3% in 1994 to 41% in 2004; however, the proportion of mesotrophic lakes significantly increased from 42.1% in 1994 to 48.1% in 2004. There was also an increase in the proportion of eutrophic lakes from 7.4% in 1994 to 9.6% in 2004 as well as a slight increase in the proportion of hypereutrophic lakes from 1.1% in 1994 to 1.3% in 2004. Provided that these two types of lakes (eutrophic and hypereutrophic) are the ones with highest biological production, even a slight increase in their proportion could have led to significant changes in the average  $CHLa_{mod}$  in the region. Overall, the chart showed that lakes of the study region became more eutrophic in the period between 1985 and 2004.

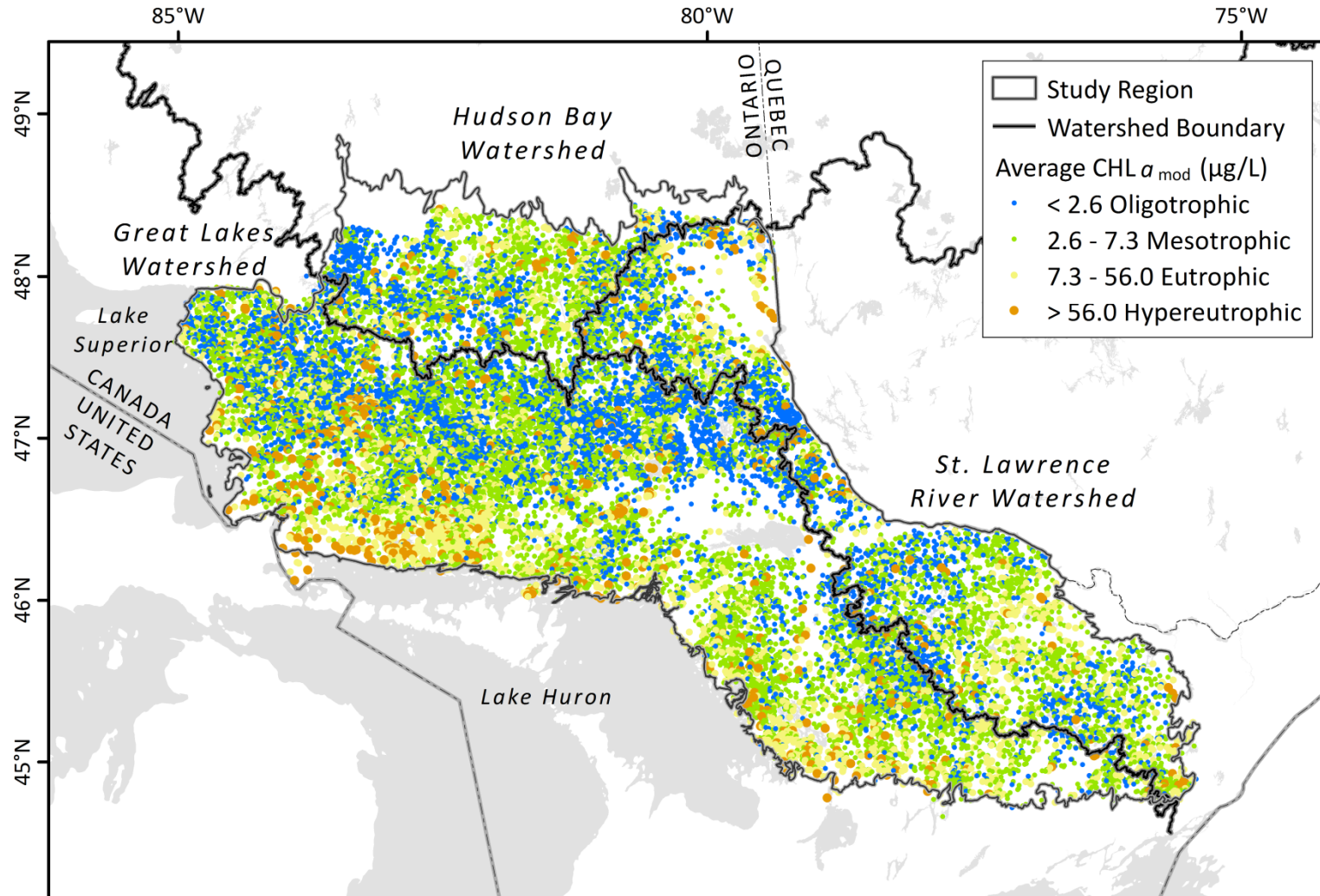


**Figure 4.5:** Map of average  $CHL a_{mod}$  ( $\mu\text{g/L}$ ) for 21,384 lakes in a 28-year record

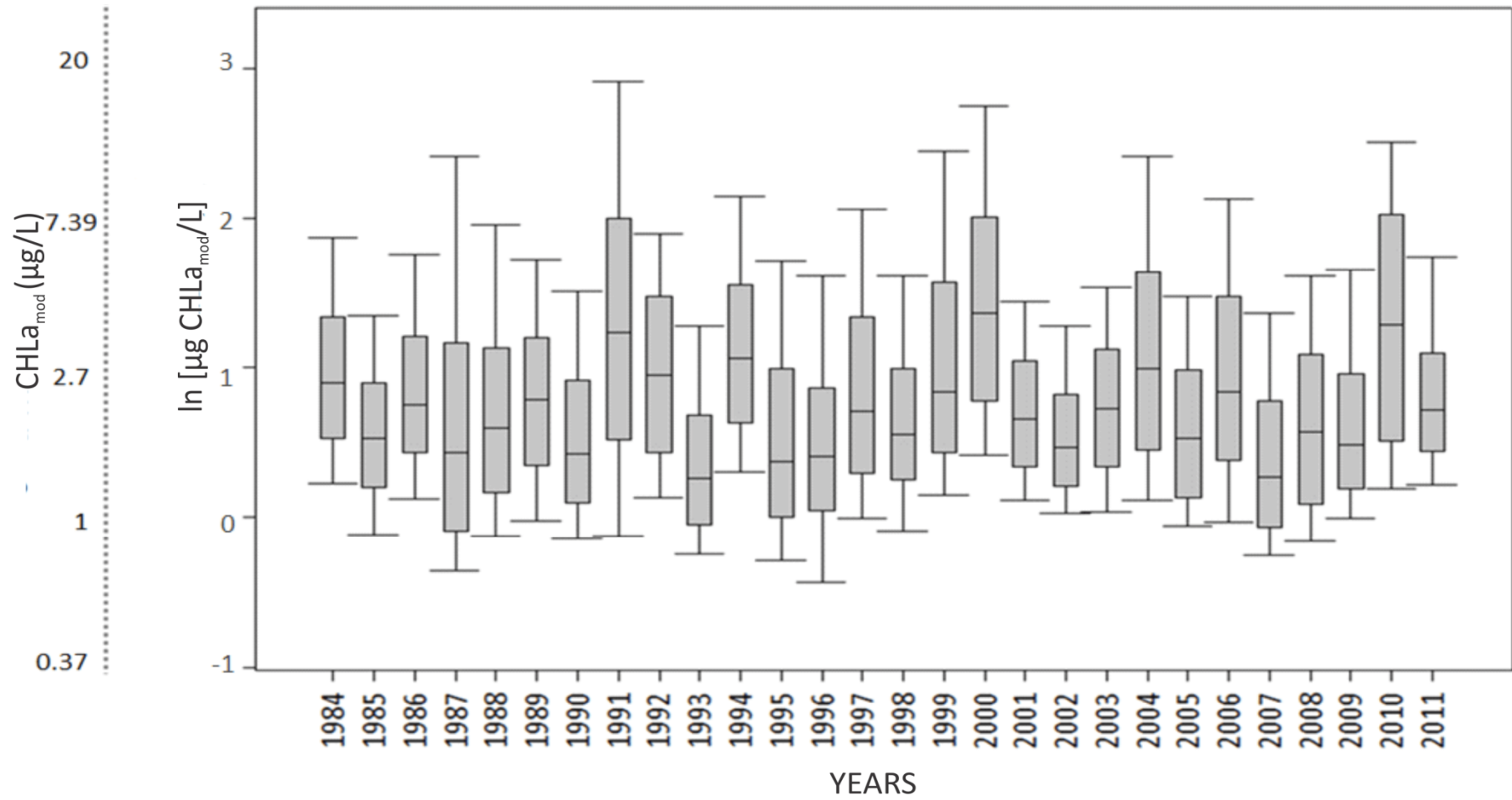


**Figure 4.6:** Time series of median CHLa<sub>mod</sub> (ln [µg CHLa<sub>mod</sub>/L]) for 6,384 lakes in a 28-year record (1984-2011) with an additional axis for CHLa<sub>mod</sub> (µg/L)



## 4.6 Decomposition of total variation into space, time and space × time components

The analysis of proportions of total variation in  $CHLa_{mod}$  revealed that the space × time interaction factor accounted for around 74.9% of total variation, while space and time factors accounted for 16.1% and 8.9% accordingly ( $p < 0.0001$ ; Figure 4.8).

In evaluating the number of years that is necessary to establish the stability of variance in  $CHLa_{mod}$  it was found that the sampling period should be not less than 12 years in order to obtain a stable variance structure (Figure 4.9). At this point the space, time and space × time interaction component levelled off and did not change significantly afterwards. It was also found that despite the fact that these factors became stable at 12 years, there was a slight increasing trend of time factor with increasing years of sampling. The space factor, in contrast, had a slight decreasing trend after 12 years.

In evaluating the number of lakes (sample size) necessary to establish the stability of variance in  $CHLa_{mod}$ , it was found that around 3,400 lakes are needed for an area the size of the study region to obtain a stable variance structure (Figure 4.10). The factors behave similarly on both plots, although not identically. The interaction between time and space factors appears more complex in Figure 4.10 (evaluating the number of samples) where they are located much closer to each other (between 10 and 20 % in proportion of total variation) and even intersect when the number of lakes reaches 3,000. The third space × time interaction factor shows a very stable pattern on both plots never dropping below 67% in total variation.

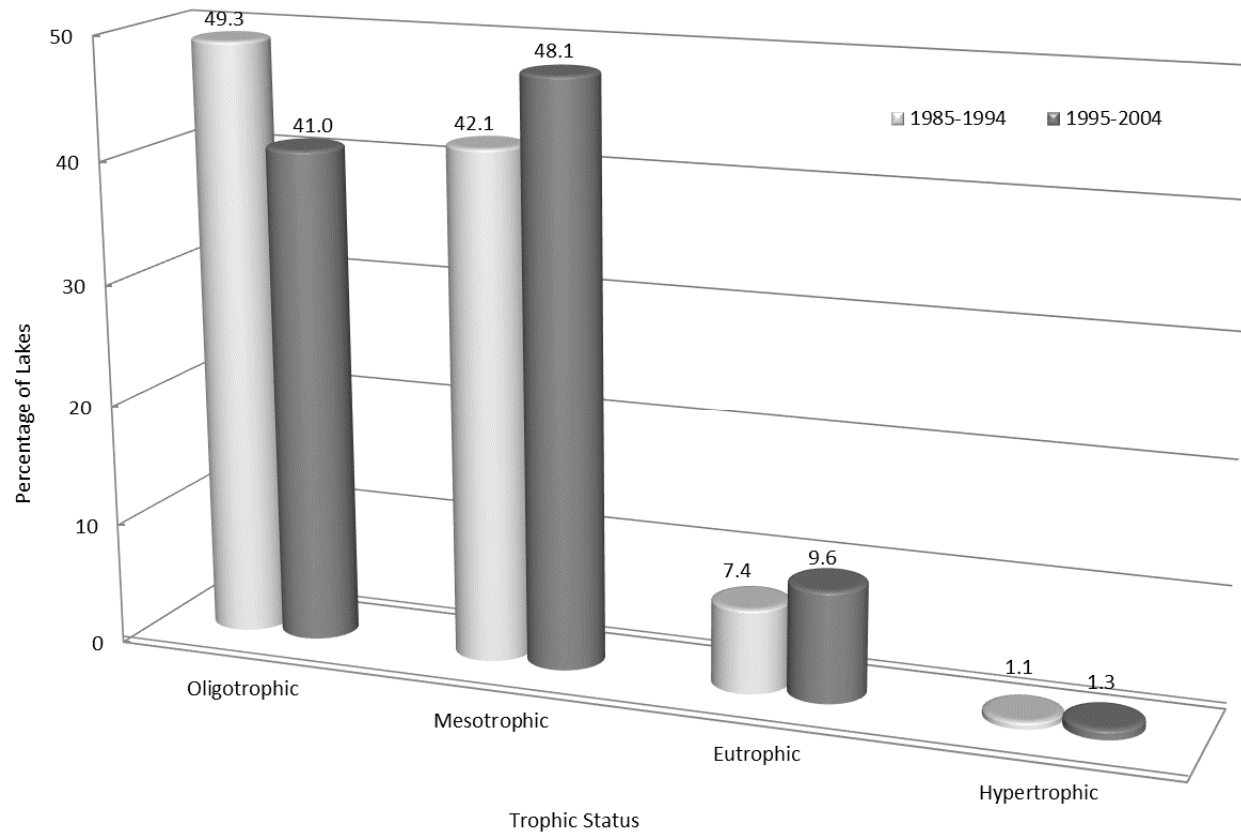


**Figure 4.7:** Comparison in distribution of trophic status of lakes (%) for two ten-year periods (1985-1994 and 1995-2004).

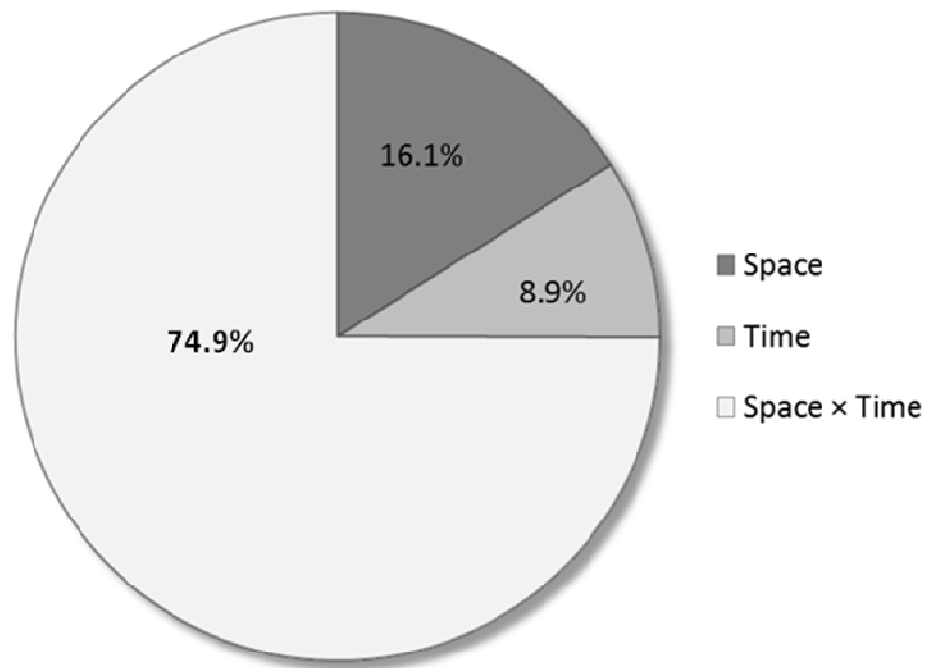


**Figure 4.8:** Sources of natural variation of  $\text{CHLa}_{\text{mod}}$  (ln [ $\mu\text{g CHLa}_{\text{mod}}/\text{L}$ ]).

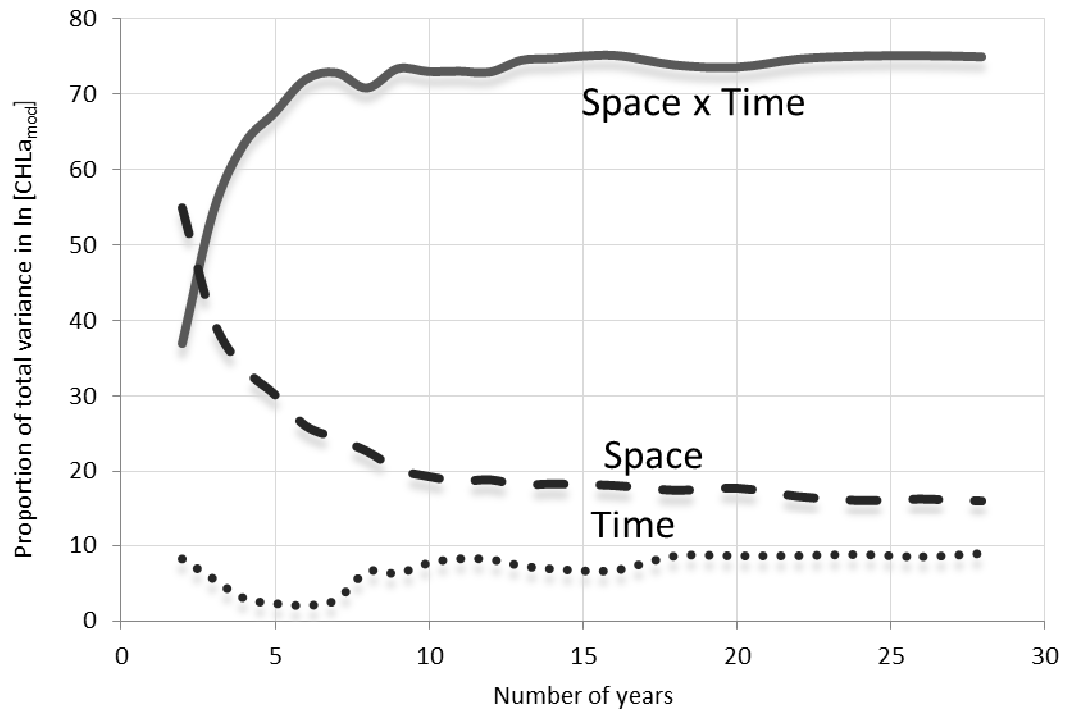


**Figure 4.9:** Number of years needed to establish the stability of variance in CHLa<sub>mod</sub> (ln [ $\mu\text{g}$  CHLa<sub>mod</sub>/L]).

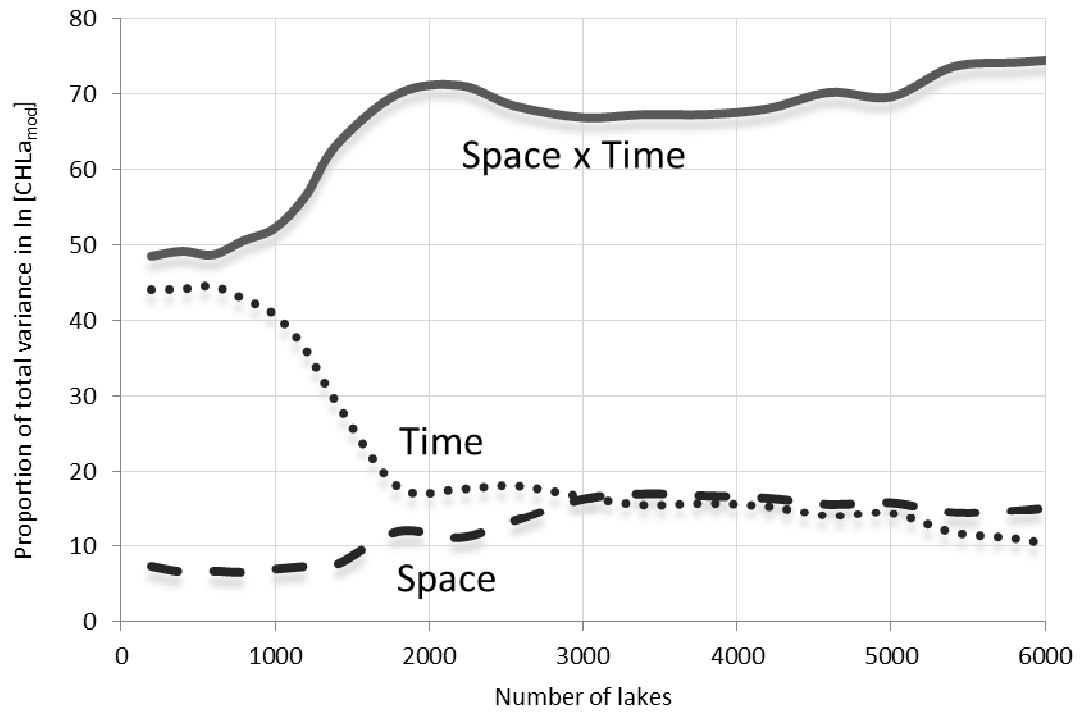


**Figure 4.10:** Number of lakes needed to establish the stability of variance in CHLa<sub>mod</sub> (ln [ $\mu\text{g}$  CHLa<sub>mod</sub>/L]).

## Chapter 5

### 5 Discussion

#### 5.1 Regression model analysis

The importance of the time window between satellite image capture and sample date (Kloiber *et al.*, 2002) was shown in this study (Figure 4.2). The fewer days between these two events the stronger the correlation (as measured in  $r^2$ ) between  $CHLa_{obs}$  and satellite reflectance. Kloiber *et al.* (2002) showed that +/-1 day was optimal for their model with a minimum sample size of 40. In this research, however, with fewer ground observations and a sharp drop in correlation (at the point of +/- 4 days), a time window of +/- 3 days was found to be optimal. There was also a concern that using *in situ* observations from different years in the same model could weaken the strength of correlation (Harma *et al.*, 2001). Our results agreed with this. Using a time window +/- 3 days and data from 2009 resulted in  $r^2 = 0.80$ , whereas using the same window with added 2010 and 2011 data led to decline in the strength with  $r^2 = 0.73$ . The subsequent abrupt drop in correlation from +/- 3 days to +/- 4 days could have been caused by different factors (e.g., the presence of outliers) not related to the year when data were sampled.

Since there were few studies conducted over a large number of lakes (i.e., hundreds or thousands; Table 1.2), it was a challenge to compare the overall results of this model with others. However, in line with the studies conducted over moderate number (tens) of lakes (Gitelson *et al.*, 1993; Allee and Johnson, 1999; Allan *et al.*, 2011), this model showed strong correlation between reflectance values from Landsat B3 and  $CHLa_{obs}$  ( $r^2=0.85$ ,  $p < 0.001$ ). The coefficients obtained by comparing  $CHLa_{mod}$  with the validation dataset (RMSE = 0.55,  $r^2 = 0.84$  and  $p < 0.0001$ ) also confirmed this. Therefore, it can be concluded that the Landsat TM and ETM+ imagery is reliable enough to be used for modelling detailed synoptic coverage of chl-a.

#### 5.2. Analysis of spatial and temporal patterns

Lake-specific variation (the space  $\times$  time interaction component) accounted for the majority of the variation in  $CHLa_{mod}$  (74.9%; Figures 4.8, 4.9 and 4.10). Such a high proportion indicates that processes occurring within lakes (lake-specific) are

most important for phytoplankton growth in the study region. These processes can be attributed to the ecology of particular phytoplankton species found in the lakes, e.g. their ability to migrate in the water column and nutrient uptake characteristics. There may be hundreds of different species of algae and cyanobacteria in a single lake that compete with each other for nutrients and better access to light (Stoermer *et al.*, 1985; Huisman *et al.*, 2004). Further, other biological factors such as predation may also have a significant effect on phytoplankton populations (Hart and Robinson, 1990).

A similar percentage in variation was found by Wiley *et al.* (1997) for two insect species (*Glossosoma nigrrior* and *Goera stylata*; 77 and 44% accordingly). However, in this research no particular species were studied. Moreover, *Glossosoma nigrrior* and *Goera stylata* are insects with well documented ecology, while it seems rather difficult to incorporate ecological characteristics for all phytoplankton species living in a lake (or several lakes) in the same paradigm. Since it is known that different phytoplankton taxa tend to dominate an environment in a different part of growing season (Wetzel, 2001), one of the feasible ways to understand the influence of the biological factor on the space  $\times$  time interaction component could be the ability to discriminate this phytoplankton taxon remotely. For example, there are techniques for distinguishing phycocyanin of cyanobacteria in large lakes from reflectance of MERIS imagery (Simis *et al.*, 2005; Kallio, 2012).

It is worth mentioning that lake-specific physical factors are of (if not the same) importance. The size and form of lakes regulate sedimentation, diffusion and mixing which in turn regulate concentrations of nutrients and suspended particulate matter which affect primary production (Hakanson, 2005). Sorichetti *et al.* (2013a) found evidence that cyanobacteria thrive in iron poor environments. This is due to their ability to migrate through the water column (Molot *et al.*, 2014) and uptake ferric iron that is unavailable to other phytoplankton species (Kranzler *et al.*, 2013). The main source of ferric iron in the temperate lakes is anoxic sediments. Anoxia in turn is highly dependent on lake morphometry and depth in particular (Molot *et al.*, 2014). By definition the space  $\times$  time interaction component also includes the error term. Unfortunately, there were no replicates in this study that would enable separation from the space  $\times$  time interaction component. Therefore, it is impossible to define what proportion within the component is taken up by the error.

Around 16% of the total variation in  $CHLa_{mod}$  was explained by the space factor (Figures 4.8, 4.9 and 4.10). This suggests that  $CHLa_{mod}$  in the lakes of the study region may be influenced by one of the landscape control elements (e.g. topography, surficial geology, forest type) or by their interaction with each other. Areas with similar geology, forest type and soils, topography and affected hydrological connectivity may have a key control on water flow and nutrient transport and accumulation (Creed *et al.*, 2002). Lakes located on the lower reaches of the local rivers or lowlands receive more nutrients than those located on uplands of watershed boundaries (Figure 4.5). Further, logging practices such as clear cutting increase erosion and lead to the changes in nutrient composition of local soils (Kreutzweiser *et al.*, 2008). These nutrients are then flushed to receiving lakes where they accumulate, likely causing an increase in phytoplankton biomass and consequent phytoplankton blooms (Devito *et al.*, 2000).

The “lake effect” (increasing productivity in proximity to the Great Lakes) found among the lakes of the study region may be attributed to the space factor. However, these lakes may be affected not so much by the neighbouring Great Lakes themselves but rather by the water flow bringing organic matter and nutrients from upstream areas. This is suggested by the fact that this pattern seems to disappear in the south-eastern portion of the region. This portion lies in the middle of the St. Lawrence River and Great Lakes Watershed, at a considerable distance from any large rivers or lakes. Moreover, the south-eastern portion is known to be much affected by human activities due to relative proximity to the most populated areas in Ontario (Baldwin *et al.*, 2000). Most of the reports on phytoplankton blooms were described for this portion as well (Winter *et al.*, 2011). Another important pattern found in the study region is a high concentration of oligotrophic lakes in the centre where they comprise an “oligotrophic belt”. In fact, this belt consists almost entirely of oligotrophic lakes with rare interruptions of mesotrophic lakes. Not surprisingly, it was found that the belt corresponds to the boundary of regional watersheds (Figure 4.5). Thus, nutrients may not accumulate in these lakes; instead they are washed out to the downstream areas via surface and groundwater streams.

A minority of variation in  $CHLa_{mod}$  was explained by the time factor (8.9%; Figures 4.8, 4.9 and 4.10). Sass *et al.* (2007) found the same result (9%) in the Alberta Boreal Plain. This is a rather interesting finding given that the Boreal Plain lies in a



considerably higher latitude than the Ontario study region (56°N vs. 46.5°N) with a generally colder (average annual temperatures +1.7°C vs. +4.5°C) and drier (average annual precipitation 469 mm vs. 990 mm) climate. The possible reason of this similarity may not be climate itself but global climate patterns occurring in these two regions. These patterns may be similar in both the Temperate Forest Biome of Ontario and the Boreal Plain of Alberta.

Climate affects the productivity and biodiversity of surface waters directly via increased temperature and radiation, changes in seasonal patterns, or intensified vertical stratification of water (Butterwick *et al.*, 2005; Elliott, 2014), and indirectly via changes in nutrient fluxes from headwater catchments (King *et al.*, 2007; Whitehead *et al.*, 2009). Climate patterns are driven both by anthropogenic climate change and by natural climatic oscillations. The patterns caused by climate change are non-stationary; i.e., their means change over time. On the other hand, patterns caused by global climatic oscillations are stationary with means repeating over time (Zhang *et al.*, 2000; Mengsitu *et al.*, 2013). Since these repeating periods can occur at scales of several decades, they may be perceived as non-stationary patterns. Thus, it is important to be able to delineate climate change from natural climatic oscillations (Sang *et al.*, 2011). Mengsitu *et al.* (2013) used wavelet analysis to develop an analytical framework allowing to deconstruct a 28-year time series of temperature in the Turkey Lakes Watershed in the Algoma Highlands into non-stationary trends and stationary cycles. The authors were able to explain the majority of variations in the time series through the prism of catchment water yield responses. This suggests that wavelet analysis may be a useful technique in explaining climate patterns (such as ones hidden in time series) and their influence on phytoplankton biomass.

Both climatic non-stationary trends and stationary cycles are likely incorporated in the times series of median  $CHL_{a_{mod}}$  for the study region (Figure 4.6). Fluctuations found in this time series may reflect year-to-year climatic variability or the North Atlantic Oscillation (Zhang *et al.*, 2000). A climatic non-stationary trend would be shown on the times series as a gradual positive or negative trend in  $CHL_{a_{mod}}$  (Blenckner *et al.*, 2007). A positive trend was expected as increasing temperature in the region should lead to higher biomass and consequently higher chl-a concentration (Downing *et al.*, 2001; O'Neil *et al.*, 2012). However, there was no significant trend towards increasing in phytoplankton biomass over the 28-year period.

This finding contradicts the work presented by Winter *et al.* (2011) who analyzed reports on phytoplankton blooms in Southern Ontario for 19 years and found significant increases in the number of phytoplankton blooms (Figure 1.1). Given that the development of a phytoplankton bloom always implies an increase in phytoplankton biomass (Paerl and Huisman, 2009) and consequently in chl-a, it is not clear why there is no direct correlation between these events. There could be three explanations for this: (1) the reports were analyzed for southern Ontario, a region that overlaps only the southern portion of the study region; (2) the reports cover the period from 1994 to 2013 while the time series presented in this region covers the period 1984-2011; and (3) there is no real increase in phytoplankton blooms but instead an increased number of reports due to increased awareness of the problem. It is outside the scope of this research to elucidate which explanation or explanations are correct. However, an attempt could be made to trace if there were any changes in the trophic status of the lakes assuming that there is an increase in the proportion of lakes with high average  $CHLa_{mod}$ .

Herein the question can be posed: was there any alteration in trophic status of lakes during the period of 1985-2004? The 21,384 lake dataset was divided into two groups corresponding to the ten-year periods of 1985-1994 (preceding the phytoplankton bloom report) and 1995-2004 (matching the first ten years of the phytoplankton bloom report). Since there were no data for 2011-2013 to organize a complete dataset corresponding to the phytoplankton bloom report, data for 2005-2011 were discarded. Data for the first year (1984) was also discarded to provide 10 continuous years of  $CHLa_{mod}$  data with the final year overlapping the first year of the phytoplankton bloom report. The proportions of lakes with different trophic statuses for each period were calculated.

There has been a shift towards eutrophication of lakes found in the period of 1985–2004 (Figure 4.7). Eutrophication trend is particularly noticeable in the pattern of oligotrophic *versus* mesotrophic lakes (with decrease in the proportion of oligotrophic lakes and almost the same increase in the proportion of mesotrophic lakes). This leads to the assumption that eutrophication of Ontario lakes started even before the 1980s and likely continues now. The finding generally correlates with the increase number of reports on phytoplankton blooms for the same period and possibly provides an insight on why more blooms are presently occurring in oligotrophic lakes.

Perhaps these lakes are no longer oligotrophic. The condition of these lakes has changed, perhaps too quickly to be perceived.

## Chapter 6

### 6 Conclusions

There is a vital need for spatially and temporally extensive datasets on chl-a concentration of numerous (hundreds and thousands) lakes, covering large spatial (>100 km<sup>2</sup>) and temporal scales (decades) to determine if the number of phytoplankton blooms increases and, if so, what processes cause this increase. In this study archived Landsat TM and ETM+ imagery was explored to model chl-a concentration in thousands of lakes across a huge region of the Temperate Forest Biome in Ontario and for the period of 28 years. It was confirmed that satellite imagery, Landsat in particular, is a unique instrument allowing to build detailed historical surveys of phytoplankton biomass that can be used for lake trophic status assessment.

The ability to distinguish between spatially and temporally extensive, and site specific (local scale) variations was shown to be of great importance. The study revealed that a majority of the variation in  $CHLa_{mod}$  (74.9%) was explained by a space  $\times$  time interaction component, leading to the conclusion that future researches should pay particular attention to the processes occurring within lakes despite the fact that regional and global-scale processes may seem to be more obvious. The spatial patterns found in the research provide an insight on the susceptibility of lakes to eutrophication and the possible directions of eutrophication processes occurring in the study region. By being able to predict the potential susceptibility of lakes to eutrophication, researchers will be able to target future monitoring and research efforts. These spatial patterns also confirm the importance of topography as a determinant of nutrient export. Topography should be considered in regulating various management strategies such as logging practices (e.g. logging in river floodplains *versus* in highlands of watershed boundaries). The temporal shift in  $CHLa_{mod}$  found between the time periods of 1985-1994 to 1995-2004 sends an important warning that eutrophication of Ontario lakes might be the reality that people should deal with. Increased number of reports on phytoplankton blooms for the period of 1995-2004 can be attributed to this process. On the other hand, we did not find any overall trend in the median  $CHLa_{mod}$  for 28 years. Therefore, future research is needed to develop new approaches for understanding the obtained time series to determine the rate and intensity of the eutrophication.

This study will form the basis for future research that will be focused on both improving the existing regression model and understanding the natural spatial and temporal patterns that were discovered in the present study. For improving the existing regression model: (1) information on new lakes with 2014  $CHL_{a_{obs}}$  will be added, covering the entire study region to allow more *in situ* data for analysis and validation; (2) Landsat ETM+ and OLI images for 2012-2014 will be retrieved and processed, so as to have complete continuous data for 30 year period (1984-2014). For understanding the spatial and temporal patterns, new analytical methods will be applied, such as: (1) digital terrain analysis techniques (Creed and Sass, 2011) to assess the relative contribution of catchments to the lake area and characterize lake-specific morphometry using digital lake bathymetry data, and (2) wavelet transformations (Mengsitu *et al.*, 2013) to distinguish between non-stationary trends and stationary cycles in climate patterns affecting the region.

## References

- Allan M. G., D. P. Hamilton, B. J. Hicks and L. Brabyn. (2011) Landsat remote sensing of chlorophyll a concentrations in central North Island lakes of New Zealand. *International Journal of Remote Sensing*. 32, 2037–2055
- Allee R.J. and J.E. Johnson (1999) Use of satellite imagery to estimate surface chlorophyll a and Secchi disc depth of Bull Shoals Reservoir, Arkansas, USA. *International Journal of Remote Sensing*. 20, 1057–72.
- Arar E.J. and G.B. Collins (1997) Method 445.0, in vitro determination of chlorophyll a and pheophytin a in marine and freshwater algae by fluorescence. *Methods for the Determination of Chemical Substances in Marine and Estuarine Environmental Matrices*, 2nd edn. National Exposure Research Laboratory, Office of Research and Development, USEPA, Cincinnati, OH, USA
- Baldwin D., J. Desloges, L. Band (2000) Physical Geography of Ontario. In, A. Perera, D. Euler and I. Thompson [eds], *Ecology of a Managed Terrestrial Landscape Patterns and Processes of Forest Landscapes in Ontario*. ISBN: 9780774807494. UBC Press. Vancouver, B.C., Canada.
- Baruah P. J., M. Tamura, K. Oki, and H. Nishimura (2001) Neural Network Modeling of Surface Chlorophyll and Sediment Content in Inland Water from Landsat Thematic Mapper Imagery Using Multi-date Spectrometer Data. *Proceedings of SPIE - The International Society for Optical Engineering* (Impact Factor: 0.2). DOI: 10.1117/12.452815
- Blenckner T., Adrian R., Livingstone D.M., Jennings E., Weyhenmeyer G.S., George D.G., Jankowski T., Jarvinen M., Aonghusa C.N., Noges T., Strailes D., Teubner K. (2007) Large-scale climatic signatures in lakes across Europe: a meta-analysis. *Global Change Biology*. 13, 1314-1326.
- Brezonik P., K. D. Menken, M. Bauer (2005) Landsat-based remote sensing of lake water quality characteristics, including chlorophyll and colored dissolved organic matter (CDOM). *Lake and Reservoir Management*. 21, 373-382

- Budd W. J. and D. S. Warrington (2004) Satellite-based Sediment and Chlorophyll a Estimates for Lake Superior. *Journal of Great Lakes Research* 30 (Suppl. 1), 459–466 International Association Great Lakes Research
- Butterwick C., S. I. Heaney, J. F. Talling (2005) Diversity in the influence of temperature on the growth rates of freshwater algae, and its ecological relevance. *Journal of Freshwater Biology* 50, 291-300.
- Canada Soil Survey Committee. 1978. Proceedings of the eighth meeting of the Canada Soil Survey Committee of Canada. Mimeographed report of the Canada Department of Agriculture, Ottawa, ON.
- Cannizzaro J. P., and K. L. Carder (2006) Estimating chlorophyll a concentrations from remote sensing reflectance in optically shallow waters. *Remote Sensing of Environment*, 101, 13- 24.
- Carleton, T. J. 2000. Vegetation responses to the managed forest landscape of central and northern Ontario. Pages 179--197 in A. H. Perera, D. L. Euler, and I. D. Thompson, editors. *Ecology of a managed terrestrial landscape: patterns and processes of forest landscapes in Ontario*. University of British Columbia Press, Vancouver, B.C., Canada.
- Carpenter D.J. and S.M. Carpenter (1983) Modelling inland water quality using Landsat data. *Remote Sensing of Environment*. 13, 345–52.
- Chander G., B. Markham, and D. Helder (2009) Summary of current radiometric calibration coefficients for Landsat MSS, TM, ETM+, and EO-1 ALI sensors. *Remote Sensing of Environment*. 113, 893–903
- Chavez P. (1996) Image-based atmospheric corrections – revisited and revised. *Photogrammetric Engineering and Remote Sensing*, 62, 1025–1036.
- Chen C.Q., P. Shi, A and Q.P. Mao. (1996) Study on modeling chlorophyll concentration of surface coastal water using TM data, *Journal of Remote Sensing*, 11(3), 168-175.
- Chen X., L. Vierling, D. Deering (2005) A simple and effective radiometric correction method to improve landscape change detection across sensors and across time. *Remote Sensing of Environment*. 98, 63 – 79

- Chipman J. W., T. M. Lillesand., J. E. Schmaltz, J. E. Leale., and M. J. Nordheim (2004) Mapping lake water clarity with Landsat images in Wisconsin, USA. *Canadian Journal of Remote Sensing*. 30, 1–7.
- Clark B., J. Suomalainen, and P. Pellikka (2010). A comparison of methods for the retrieval of surface reflectance factor from multitemporal SPOT HRV, HRVIR, and HRG multispectral satellite imagery. *Canadian Journal of Remote Sensing*. 36 (4), 397–411.
- Creed I. F., C. G. Trick, L. E. Band, and I. K. Morrison (2002) Characterizing the spatial heterogeneity of soil carbon and nitrogen pools in the Turkey Lakes Watershed: A comparison of regression techniques, *Water Air Soil Pollution Focus*. 2, 81–102.
- Creed I. F., G. Z. Sass (2011) Digital terrain analysis approaches for tracking hydrological and biogeochemical pathways and processes in forested landscapes. In *Forest Hydrology and Biogeochemistry: Synthesis of Past Research and Future Directions*, Levia D., Carlyle-Moses D., Tanaka T. (eds). Springer-Verlag: New York, USA
- Dekker A. G., and W. M. Peters (1993) The use of Thematic Mapper for the analysis of eutrophic lakes: A case study in The Netherlands. *International Journal of Remote Sensing*. 14, 799-821.
- Dekker A.G., R.J. Vos and S.W.M. Peters (2002) Analytical algorithms for lake water TSM estimation for retrospective analyses of TM and SPOT sensor data. *International Journal of Remote Sensing*. 23, 15–35.
- Devito K. J., I. F. Creed, T. Gan, C. A. Mendoza, R. Petrone, U. Silins and B. Smerdon (2005). A framework for broad scale classification of hydrologic response units on the Boreal Plain: Is topography the last thing to consider? *Hydrological Processes*, 19, 1705–1714.
- Downing J., S. Watson and E. McCauley (2001) Predicting cyanobacteria dominance in lakes. *Canadian Journal of Fisheries and Aquatic Sciences*, 58, 1905–1908.
- El-Alem A., K. Chokmani, I. Laurion, and S. E. El-Adlouni. (2014). An Adaptive Model to Monitor Chlorophyll a in Inland Waters in Southern Quebec Using Downscaled MODIS Imagery. *Remote Sensing*. 6, 6446-6471.
- Elliott J.A. (2010) The seasonal sensitivity of cyanobacteria and other phytoplankton to changes in flushing rate and water temperature. *Global Change Biology*. 16, 864-876



- Foley J., DeFries R., Asner G., Barford C., Bonan G., Carpenter S., F., S. Chapin, M. T. Coe, G. C. Daily, H. K. Gibbs, J. H. Helkowski, T. Holloway, E. A. Howard, C. J. Kucharik, C. Monfreda, J. A. Patz, I. C. Prentice, N. Ramankutty, P. K. Snyder (2005) Global consequences of land use. *Science*. 309, 570–574.
- Fraser R.N. (1998) Hyperspectral remote sensing of turbidity and chlorophyll a among Nebraska Sand Hills lakes. *International Journal of Remote Sensing*. 19, 1579–1589.
- Frazier P., K. Page, J. Louis, S. Briggs, A. I. Robertson (2003) Relating wetland inundation to river flow using Landsat TM data. *International Journal of Remote Sensing*. 24, 3755–3770
- Furby S.L. and N.A. Campbell (2001) Calibrating images from different dates to “like-value” digital counts. *Remote Sensing of Environment*. 77, 186–196.
- Giardino C., M. Bresciani, D. Stroppiana, A. Oggioni, G. Morabito. (2014) Optical remote sensing of lakes: an overview on Lake Maggiore. *Journal of Limnol.* 73 (1), 201-214
- Gitelson A., G. Garbuzov, F. Szilagy, K.-H. Mittenzwey, A. Karnieli, and A. Kaiser (1993) Quantitative remote sensing methods for real-time monitoring of inland water quality. *International Journal of Remote Sensing*, 14, 1269-1295
- Glibert P.M., D.M. Anderson, P. Gentien, E. Graneli and K.G. Sellner (2005) The global, complex phenomena of harmful phytoplankton blooms. *Oceanography*. 18, 136–147.
- Hakanson L. (2005) The Importance of lake morphometry for the structure and function of lakes. *International Review of Hydrobiology*. 90 (4), 433– 461.
- Harma P., J. Vepsäläinen, T. Hannonen, T. Pyhälä, J. Kamari, K. Kallio, K. Eloheimo, S. Koponen (2001) Detection of water quality using simulated satellite data and semi-empirical algorithms in Finland. *The Science of the Total Environment*. 268, 107-121
- Hart D.D. and Robinson C.T. (1990) Recourse limitation in a stream community: effects of phosphorus enrichment on periphyton and grazers. *Ecology*. 71, 1494-1502.
- Havens E. K. (2008) Cyanobacterial Harmful Algal Blooms: State of the Science and Research Needs. *Advances in Experimental Medicine and Biology*. 619, 733-748.

- Hellweger F. L., P. Schlosser, U. Lall, and J. K. Wessel (2004) Use of satellite imagery for water quality studies in New York Harbor. *Estuarine, Coastal and Shelf Science*. 61, 437- 448
- Hicks B. J., G. A. Stichbury, L. K. Brabyn, M. G. Allan, S. Ashraf (2013) Hindcasting water clarity from Landsat satellite images of unmonitored shallow lakes in the Waikato region, New Zealand. *Environment Monitoring Assess.* 185, 7245–7261
- Huisman J. J., J. M. Sharples, P. M. Stroom, W. A. Visser, Jolanda M. H. Kardinaal, Verspagen and B. Sommeijer (2004) Changes in turbulent mixing shift competition for light between phytoplankton species. *Ecology*. 85(11), 2960–2970
- Kallio K., Attila J., Härmä P., Koponen S., Pulliainen J., Hyttiäinen U.M., Pyhälähti T. (2008) Landsat ETM images in the estimation of seasonal lake water quality in boreal river basins. *Environmental Management*, 42, 511–522.
- Karakaya N., F. Evrendilek, G. Aslan, K. Gungor, and D. Karakas (2011) Monitoring of lake water quality along with trophic gradient using Landsat data. *International Journal of Environmental Science and Technology*. 8 (4), 817–822.
- King K.W., J.C. Balogh, R.D. Harmel (2007) Nutrient flux in storm water runoff and base flow from managed turf. *Environnemental Pollution*. 150, 321-328.
- Kloiber S. M., P. L. Brezonik, L. G. Olmanson and M. E. Bauer (2002) A procedure for regional lake water clarity assessment using Landsat multispectral data. *Remote Sensing of Environment*. 82, 38–47.
- Kreutzweiser D.P., P.W. Hazlett., and J.M. Gunn (2008) Logging impacts on the biogeochemistry of boreal forest soils and nutrient export to aquatic systems: A review. *Environment Reviews*. 16, 157–179. DOI:10.1139/A08-006.
- Kranzler C., M. Rudolf, N. Keren and E. Schleiff (2013) Iron in cyanobacteria. *Advances in Botanical Research*. 65, 57–105.
- Kutser T. (2009) Passive optical remote sensing of cyanobacteria and other intense phytoplankton blooms in coastal and inland waters. *International Journal of Remote Sensing*, 30 (17), 4401–4425
- Lathrop R.G., T.M. Lillesand and B.S. Yandell (1991) Testing the utility of simple multirate Thematic Mapper calibration algorithms for monitoring turbid inland waters. *International Journal of Remote Sensing*. 12, 2045–2063.

- Lewis W.M. (1978) Comparison of temporal and spatial variation in the zooplankton of a lake by means of variance components. *Ecology*. 59, 666-671
- Liu Y., M. A. Islam and J. Gao (2003). Quantification of shallow water quality parameters by means of remote sensing. *Progress in Physical Geography*. 27, 24–43.
- Lu D, P. Mausel, E. Brondizio and E. Moran. (2002) Assessment of atmospheric correction methods for Landsat TM data applicable to Amazon basin LBA research. *International Journal of Remote Sensing*. 23, 2651-2671.
- Mahiny A.S., and B. J. Turner (2007) A Comparison of Four Common Atmospheric Correction Methods. *Photogrammetric Engineering & Remote Sensing*. 73 (4), 361–368.
- Mather P. and B. Tso (2009) Classification methods for remotely sensed data. 2<sup>nd</sup> Ed. 376. CRC press, New York, USA
- Mayo M., A. Gitelson, Y.Z. Yacobi and Ben Avraham Z. (1995) Chlorophyll distribution in Lake Kinneret determined from Landsat Thematic Mapper data. *International Journal of Remote Sensing*. 16, 175–82.
- McKenney D. W., M. F. Hutchinson, P. Papadopol, K. Lawrence, J. Pedlar, K. Campbell, E. Milewska, R. F. Hopkinson, D. Price, and T. Owen (2011) Customized Spatial Climate Models for North America. *Bull. American Meteorological Society*. 92, 1611–1622.
- McCullough I. M., C. S. Loftin, S. A. Sader. (2012) Combining lake and watershed characteristics with Landsat TM data for remote estimation of regional lake clarity. *Remote Sensing of Environment*. 123, 109–115
- Molot L. A., S. B. Watson, I. F. Creed, C. G. Trick, S. K. McCabe, M. J. Verschoor, R. J. Sorichetti, C. Powe, J. J. Venkiteswaran and S. L. Schiff. (2014) A novel model for cyanobacteria bloom formation: the critical role of anoxia and ferrous iron. *Freshwater Biology*, 59, 1323–1340
- Nelson Stacy A.C., P. A. Soranno, K. S. Cheruvilil, S. A. Batzli and D. L. Skole (2003) Regional assessment of lake water clarity using satellite remote sensing. Papers from Bolsena Conference. Residence time in lakes: Science, Management, Education *Journal of Limnology*, 62 (Suppl. 1), 27-32

- Olmanson L. G., P. L. Brezonik, and M. E. Bauer. (2013) Geospatial and Temporal Analysis of a 20-Year Record of Landsat-Based Water Clarity in Minnesota's 10,000 Lakes. *Journal of the American Water Resources Association (JAWRA)* 50(3), 748-761. DOI: 10.1111/jawr.12138
- O'Neil J.M., W. T. Davis, A.M. Burford, J.C. Gobler (2012) The rise of harmful cyanobacteria blooms: The potential roles of eutrophication and climate change. *Harmful algae*, 14, 313-334.
- Ontario Geological Survey (2003) Surficial geology of southern Ontario, Misc. Release-Data 128, Toronto, ON, Canada.
- Paerl H.W. and J. Huisman (2009) Climate change: a Catalyst for global expansion of harmful cyanobacterial blooms. *Environmental Microbiology Reports*, 11, 27-37.
- Paerl H.W. and J. V. Paul (2012) Climate change: Links to global expansion of harmful Cyanobacteria. *Water research*, 46, 1349-1363
- Paul V.J. (2008) Global warming and cyanobacterial harmful phytoplankton blooms. *Advances in Experimental Medicine and Biology*, 619, 239-257
- Perera A.H. and D.J.B. Baldwin (2000) Spatial patterns in the managed forest landscape of Ontario. Pages 74-99. In: A.H. Perera, D.L. Euler and I.D. Thompson (editors). *Ecology of a Managed Terrestrial Landscape: Patterns and Processes in Forest Landscapes of Ontario*. UBC Press, Toronto.
- Pulliainen J., K. Kallio, K. Eloheimo, S. Koponen, H. Servomaa, T. Hannonen, S. Tauriainen, M. Hallikainen (2001) A semi-operative approach to lake water quality retrieval from remote sensing data. *Science of the Total Environment*. 268, 79-93.
- Richardson L. (1996) Remote Sensing of Algal Bloom Dynamics. *BioScience*, 46 (7), 492-501.
- Ritchie J. C., C. M. Cooper, and F. R. Schiebe (1990) The relationship of MSS and TM digital data with suspended sediments, chlorophyll and temperature in Moon Lake, Mississippi. *Remote Sensing of Environment*. 33, 137-148.
- Rodríguez Y. C., A. El. Anjoumi, J. A. Domínguez Gómez, D. Rodríguez Pérez, E. Rico. (2014) Using Landsat image time series to study a small water body in Northern Spain. *Environ Monitoring Assess.* 186, 3511-3522. DOI 10.1007/s10661-014-3634-8

- Sang Y.F., D. Wang, J.-C. Wu, Q.-P. Zhu, L. Wang (2011) Wavelet-Based Analysis on the Complexity of Hydrologic Series Data under Multi-Temporal Scales. *Entropy*, 13, 195-210.
- Sass G, I.F. Creed, S.E. Bayley, and K.J. Devito. (2007) Understanding variation in trophic status of lakes on the Boreal Plain: a 20 year retrospective using Landsat TM imagery. *Remote Sensing of Environment*.109, 127-141.
- Sass G. Z., I. F. Creed, S. E. Bayley, and K. J. Devito (2008) Inter-annual variability in trophic status of shallow lakes on the Boreal Plain: Is there a climate signal? *Water Resources Research*, 44 (8). DOI:10.1029/2007WR006310
- Schott J. R., C. Salvaggio, and W. J. Volchok (1988). Radiometric scene normalization using pseudoinvariant features. *Remote Sensing of Environment* . 26, 1 – 16.
- Shunlin L., F. Hongliang, and C. Mingzhen (2001). Atmospheric Correction of Landsat ETM+ Land Surface Imagery - Part I: Methods”, *IEEE Transactions on geoscience and remote sensing*. 39 (11), 2490-2498
- Simis S. G., S. W. Peters, and H. Gons (2005). Remote Sensing of the cyanobacterial pigment phycocyanin in turbid inland water. *Limnology and Oceanography*, 50, 237-245
- Sorichetti R.J., I.F. Creed and C.G. Trick (2013a) Evidence for iron-regulated cyanobacterial predominance in oligotrophic lakes. *Freshwater Biology*, 59 (4), 679-691. DOI:10.1111/fwb.12295
- Sorichetti R. J. (2013b) Iron-Regulated Cyanobacterial Predominance and Siderophore Production in Oligotrophic Freshwater Lakes. University of Western Ontario - Electronic Thesis and Dissertation Repository. Paper 1825.
- Stoermer E. F., J. A. Wolin, C. L . Schelske, D. J. Conley (1985) An assessment of ecological changes during the recent history of lake Ontario based on siliceous algal microfossils preserved in the sediments 1, 2. *Journal of Phycology*. 21(2), 257-276.
- Svab E., A. N. Tyler, T. Preston, M. Presing, and K. V. Balogh (2005) Characterizing the spectral reflectance of algae in lake waters with high suspended sediment concentrations. *International Journal of Remote Sensing*. 26, 919–928.
- Tebbs E.J., J.J. Remedios, D.M. Harper (2013) Remote sensing of chlorophyll-a as a measure of cyanobacterial biomass in Lake Bogoria, a hypereutrophic, saline–

- alkaline, flamingo lake, using Landsat ETM+. *Remote Sensing of Environment*. 135, 92–106
- Vincent R.K., X. Qin, R.M.L. McKay, J. Miner, K. Czajkowski, J. Savino, T. Bridgeman (2004) Phycocyanin detection from Landsat TM data for mapping cyanobacterial blooms in Lake Erie. *Remote Sensing of Environment*. 89, 381–392
- Wetzel R. (2001) *Limnology: Lake and river ecosystems*. 3d ed. San Diego, CA: Acad. Press, USA
- Wiley M. J., S. L. Kohler, and P.W. Seelbach (1997) Reconciling landscape and local views of aquatic communities: Lessons from Michigan trout streams. *Freshwater Biology*. 37, 133–148.
- Winter J.G., A. M. DeSellas, R. Fletcher, L. Heintsch, A. Morley, L. Nakamoto, K. Utsumi (2011) Algal blooms in Ontario, Canada: Increases in reports since 1994. *Lake and Reservoir Management*. 27, 107-114.
- Whitehead P. G., R. L. Wilby, R. W. Battarbee, M. Kernan, A. J. Wade (2009) A review of the potential impacts of climate change on surface water quality, *Hydrological Sciences Journal*, 54, 101–123.
- Zhang X., L. A. Vincent, W.D. Hogg, and A. Niitsoo (2000) Temperature and precipitation trends in Canada during the 20th century, *Atmosphere-Ocean*, 38 (3), 395-429, DOI: 10.1080/07055900.2000.9649654
- Zhu Z., C.E. Woodcock (2012) Object-based cloud and cloud shadow detection in Landsat imagery. *Remote Sensing of Environment*. 118, 83-94

## Curriculum Vitae

**Name:** Aleksey Paltsev

**Post-secondary Education and Degrees:** Western University  
London, Ontario, Canada  
2013 - 2015 MSc. Candidate

Tambov State University  
Tambov, Russia  
1997 - 2002 Diploma in Geography

**Related Work Experience**

Graduate Teaching Assistant  
Western University  
2013 – present

Administrative Assistant  
UNESCO Moscow Office, Russia  
2011 – 2012

Scientific Associate  
Natural Biosphere Reserve Brajnsky Forest, Russia  
2002 – 2012

Research Assistant  
Institute of Geography of Russian Academy of Science  
2002 - 2005

### **Presentations:**

Paltsev A, Creed I.F. (2013) Predicting susceptibility of oligotrophic lakes in Ontario to formation of cyanobacteria blooms. Theme 2 meeting for the NSERC Canadian Network for Aquatic Ecosystem Services. Vancouver, BC, Canada. December 2013.

Paltsev A. (2009) Population organization of deciduous forest species in flood-lands of a small river. The 12th International Botanical Conference in S.-Petersburg, Russia. June 2009

Paltsev A. (2002) The long-term prognosis of flood-lands associations' development in nature reserve "Bryanskiy Les". The 45th Symposium of the International Associations for Vegetation Science. Porto Alegre, Brazil, March, 2002.

**Publications:**

Paltsev A. (2009) Population organization of deciduous forest species in flood-lands of a small river. Materials of the 12th International Botanical Conference in S.-Petersburg. 12: 101-102.

Paltsev A. (2002) The long-term prognosis of flood-lands associations' development in nature reserve "Bryanskiy Les". Materials of the 45th Symposium of the International Associations for Vegetation Science. Porto Alegre (Brazil). 45 (Mar. 3-8): 26-27